國立臺灣大學工學院機械工程學系

博士論文

Department of Mechanical Engineering

College of Engineering

National Taiwan University

Doctoral Dissertation

一種利用灰階強度微分值之指紋方向場估算法

An Effective Fingerprint Orientation Field Estimation Method Using Differential Values of Grayscale Intensity

沈庭緯

Ting-Wei Shen

指導教授: 吳文方 博士

Advisor: Wen-Fang Wu, Ph.D.

中華民國 112 年 8 月

August 2023

doi:10.6342/NTU202302201

doi:10.6342/NTU202302201

國立臺灣大學博士學位論文
口試委員會審定書
PhD DISSERTATION ACCEPTANCE CERTIFICATE
NATIONAL TAIWAN UNIVERSITY

一種利用灰階強度微分值之指紋方向場估算法

An Effective Fingerprint Orientation Field Estimation Method Using Differential Values of Grayscale Intensity

本論文係沈庭緯君(D05543008)在國立臺灣大學機械工程所完成之博士學位論文，於民國 112 年 7 月 4 日承下列考試委員審查通過及口試及格，特此證明。

The undersigned, appointed by the Department / Institute of Mechanical Engineering on 4 / 7 / 2023 have examined a PhD dissertation entitled above presented by Shen, Ting-Wei (D05543008) candidate and hereby certify that it is worthy of acceptance.

口試委員 Oral examination committee:

吳文方
（指導教授 Advisor）

楊宏智

李中裕

張恆華

丁肇隆

張[illegible]源

李[illegible]

系主任/所長 Director: 林沛群

doi:10.6342/NTU202302201

doi:10.6342/NTU202302201

Acknowledgements

首先感謝吳文方教授無私的指導，學長曾宗亮教授學業上的分享，徐茂修教授和與沈俊旭教授論文上的建議，也很感謝丁肇隆教授，張恆華教授，楊宏智教授，張敬源教授，和我碩班的老師李敏鴻教授及我的前輩李中裕博士願意擔任我的論文口試委員，並給予我寶貴且實用的意見及做研究的心得分享。最後感謝我的家人爸爸沈永豐先生、媽媽黃怡菁女士、弟弟沈正評，還有我的老婆王品方和寶寶沈承勳平時給我加油打氣，謝謝你們的支持。謹以此文，獻給你們。

doi:10.6342/NTU202302201

doi:10.6342/NTU202302201

摘要

在現今社會指紋識別技術已被廣泛應用於各種領域，包括門禁系統、法醫調查和海關管控等。然而低品質的指紋影像可能會影響指紋特徵識別的準確度。因此需要利用指紋影像增強技術來克服這個問題，比如 Gabor 濾波器就是最常見指紋影像增強技術，而 Gabor 濾波器需要可靠的方向場估算來確保影像增強的效果。在這篇論文中，我們介紹一種利用灰階強度微分值之指紋方向場估算法，並利用高斯模糊和高斯雜訊降低指紋影像品質，來檢驗所提出的演算法的準確性和可靠性。實驗結果顯示，在低品質的指紋影像中，本文所提演算法在指紋方向場估算的可靠性方面比基於梯度演算法和基於功率頻譜密度演算法更好。尤其是在有雜訊的指紋影像中，本文演算法指紋方向場估算可靠性比基於梯度演算法和基於功率頻譜密度演算法分別提高了 6.46%和 32.93%。

關鍵字：指紋、方向場估算、指紋方向場估算–梯度法、Gabor 濾波器

doi:10.6342/NTU202302201

doi:10.6342/NTU202302201

Abstract

Fingerprint identification technologies are widely used for various applications, including access control systems, forensic investigations, and border security. However, low-quality fingerprint images may affect the accuracy of fingerprint identification. Therefore, fingerprint image enhancement, such as the Gabor filter, is necessary and the Gabor filter requires a reliable orientation field estimation to ensure the result of image enhancement. In this study, we introduce an orientation field estimation algorithm based on differential values of grayscale intensity and examine the accuracy and reliability of the proposed algorithm by applying it to fingerprint images processed using the Gaussian blurring and the Gaussian white noise process. The experimental results indicate that the orientation field estimation reliability of the proposed algorithm is higher than the gradient-based method and the power spectrum density-based method in low quality fingerprints. The proposed algorithm is especially useful in noisy fingerprint images, where the orientation field estimation reliability of the algorithm is 6.46% and 32.93% higher than the gradient-

doi:10.6342/NTU202302201

based method and the power spectrum density-based method, respectively.

Keywords: Fingerprint, Orientation Field Estimation, The Gradient-based Method, The Gabor Filter

doi:10.6342/NTU202302201

Contents

	Page
Verification Letter from the Oral Examination Committee	**i**
Acknowledgements	**iii**
摘要	**v**
Abstract	**vii**
Contents	**ix**
List of Figures	**xi**
List of Tables	**xiii**
Nomenclature	**xv**
Chapter 1 Introduction	**1**
1.1 Introduction	1
1.2 Related methods	8
1.2.1 The gradient-based method	8
1.2.2 The PSD-based method	9
Chapter 2 Methodology	**13**
2.1 Differential values of grayscale intensity in each orientation	13
2.2 Image partition	18
2.3 Image convolution	20

doi:10.6342/NTU202302201

2.4 Orientation field estimation (index, matrices) 25

2.5 Image reconstruction 25

Chapter 3 Experiments and Results **29**

3.1 Database 34

3.2 Experiment 1: Accuracy assessment in clear fingerprint images . . . 34

3.3 Experiment 2: Accuracy assessment in blurred fingerprint images . . 39

3.4 Experiment 3: Accuracy assessment in noisy fingerprint images . . . 46

Chapter 4 Conclusions **55**

Chapter 5 Future Work **57**

References **59**

Appendix — Biography and Publication **65**

.1 Biography 65

.2 Publication 65

doi:10.6342/NTU202302201

List of Figures

1.1 Fingerprint image and fingerprint image enhancement with the Gabor filter. (a) Original fingerprint image; (b) Fingerprint image enhancement with the Gabor filter 5

1.2 Gabor filter bank. 6

1.3 Fingerprint image and fingerprint image distortions with the Gabor filter. (a) Original fingerprint image; (b) Fingerprint image distortions with the Gabor filter (wrong orientation) 7

1.4 Fingerprint images and power spectrum density of fingerprint images. (a) The fingerprint image-a; (b) The PSD of fingerprint image-a; (c) The fingerprint image-b; (d) The PSD of fingerprint image-b 11

2.1 Schematic view of 16 orientations of a fingerprint image. 15

2.2 Line graphs of grayscale intensities of straight lines in the 16 orientations shown in Figure 2.1. 16

2.3 The proposed OF estimation process. 17

2.4 Schematic view of fingerprint image partition. 19

2.5 A example of image convolution process. 22

2.6 The convolution kernels of the 16 orientations. 23

2.7 The Prewitt filter kernels. (a) Kernel of G_x; (b) Kernel of G_y 24

2.8 Fingerprint image and fingerprint OF. 27

3.1 Fingerprint image samples for experiments: (a) Original Sample; (b) Blurred Sample; (c) Noisy Sample 32

3.2 LabVIEW source code and GUI: (a) Source code; (b) GUI 33

doi:10.6342/NTU202302201

3.3 Deviations in the estimated OF between the proposed method/the PSD-based method and the gradient-based method on clear fingerprint images (1,500 blocks). 36
3.4 Deviations in the estimated OF between the proposed method/the PSD-based method and the gradient-based method on clear fingerprint images (1,500 blocks) by location. 37
3.5 OF estimation of each fingerprint block on clear fingerprint images using the proposed method, the gradient-based method and the PSD-based method (1,500 blocks). 38
3.6 The Gaussian blurring kernel. 41
3.7 Deviations in estimated OF between clear and blurred fingerprint images (1,500 blocks). 42
3.8 OF estimation of each fingerprint block on blurred fingerprint images using the proposed method (1,500 blocks). 43
3.9 OF estimation of each fingerprint block on blurred fingerprint images using the gradient-based method (1,500 blocks). 44
3.10 OF estimation of each fingerprint block on blurred fingerprint images using the PSD-based method (1,500 blocks). 45
3.11 Deviations in estimated OF between clear and noisy fingerprint images (1,500 blocks). 48
3.12 OF estimation of each fingerprint block on noisy fingerprint images using the proposed method (1,500 blocks). 49
3.13 OF estimation of each fingerprint block on noisy fingerprint images using the gradient-based method (1,500 blocks). 50
3.14 OF estimation of each fingerprint block on noisy fingerprint images using the PSD-based method (1,500 blocks). 51

doi:10.6342/NTU202302201

List of Tables

3.1 The performance of the proposed OF estimation method, the gradient-based method, and the PSD-based method on blurred and noisy fingerprint images. 52

3.2 Advantages and disadvantages of the proposed method and the classic OF estimation methods. 53

doi:10.6342/NTU202302201

doi:10.6342/NTU202302201

Nomenclature

OF	Orientation field
PSD	Power spectrum density
FFT	Fast fourier transform
LabVIEW	Laboratory virtual instrument engineering workbench
GUI	Graphical user interface
VI	Virtual instrument
VDM	Vision development module
CNN	Convolutional neural network
RNN	Recurrent neural network
G_x	The gradient of x-direction
G_y	The gradient of y-direction
ϕ	The gradient angle

doi:10.6342/NTU202302201

$\overline{\phi}$	The averaged gradient angle
θ	The orientation angle
G_{sx}	The squared gradient x-direction
G_{sy}	The squared gradient y-direction
$\overline{G}_{sx}$	The averaged squared gradient x-direction
$\overline{G}_{sy}$	The averaged squared gradient y-direction
θ_B	The direction of orientation field for a block B
g	The grayscale value of the image
k	The convolution kernel
f	The convolution result
m, n	The center pixel to perform convolution
i, j	The corresponding pixels covered in the kernel
M, N	The size of fingerprint image.
I, J	The size of kernel.
F	The sum of the absolute grayscale values for each block after convolution with orientation kernel
F_{min}	The minimum Y value which implies this orientation is closest to fingerprint orientation

doi:10.6342/NTU202302201

Chapter 1 Introduction

1.1 Introduction

Fingerprints are widely recognized as one of the most effective and reliable personal identification [1, 19, 23, 35]. Their usefulness arises from two main factors. Firstly, fingerprints are unique and remain unchanged throughout a person's life, making them an ideal biometric indicator of an individual's identity [3, 33]. Secondly, fingerprints have the highest reliability of all biometric indicators, making them a preferred choice for use in various fields [8, 29]. Fingerprint identification technology is commonly used in forensic investigations by law enforcement authorities to identify suspects or link evidence to a specific individual [17, 18]. This is possible because fingerprints leave behind unique and identifiable impressions on surfaces they come into contact with. The use of fingerprint identification in criminal investigations has proven to be highly effective, leading to the successful prosecution of many criminals. In addition to forensic investigations, fingerprint identification technologies are also utilized in other fields, such as border control and access control systems for secure facilities. In border control, fingerprints can be used to verify the identity of travelers, while in access control systems, they can be used to restrict access to authorized personnel only. The unique and immutable nature of fingerprints, combined with their high reliability, makes them a valuable tool for personal

doi:10.6342/NTU202302201

identification in various fields, including law enforcement, border control, and access control systems.

Fingerprint matching is a crucial task in forensic investigations and identification systems. It involves the extraction of fingerprint features from imaging, which can be either global or local [11]. However, the accuracy and reliability of these methods heavily depend on the quality and integrity of the fingerprint images [4, 25]. To improve the quality of fingerprint images, fingerprint enhancements are often employed, which can help display the fingerprint features more clearly and extract them more accurately [2, 24]. Various techniques and methods are available for fingerprint enhancement. Current fingerprint image enhancement algorithms aim to reduce noise and increase contrast in fingerprint images. Fingerprint enhancements can significantly impact the accuracy of fingerprint matching, especially when dealing with low-quality or degraded fingerprint images.

The Gabor filter is a well-known classic algorithm that can effectively enhance fingerprint images [40], also known as a Gabor wavelet or Gabor kernel (refer to Fig 1.1). It is named after Dennis Gabor, a Nobel Prize-winning physicist who first described this filter in the 1940s. The Gabor filter is commonly used in computer vision applications such as image enhancement. It is especially useful for patterns that vary in both orientation and frequency, such as lines and edges in an image, therefore can help extract fingerprint features more accurately from degraded fingerprint images, thus enhancing the overall performance of fingerprint identification systems. The Gabor filter is a type of linear filter that is designed to mimic the receptive field of simple cells in the visual cortex of the brain. These cells are known to have specific orientation tuning, which means they are sensitive to certain orientations of visual stimuli. By using a Gabor filter image pro-

doi:10.6342/NTU202302201

cessing algorithms can mimic this orientation selectivity, and use it to analyze the spatial frequency content of an image at different orientations and scales. The Gabor filter is created by modulating a Gaussian function with a sinusoidal wave. The Gaussian function provides the filter with a spatial localization, meaning that it only responds to features in a small region of the image. The sinusoidal wave provides the filter with a frequency selectivity, meaning that it only responds to features with a certain spatial frequency.

The Gabor filter have 5 main variables, namely, the wavelength of the sinusoidal factor, the orientation of the Gabor filter, the phase offset, the standard deviation of the Gaussian function and the spatial aspect ratio which specifies the ellipticity of the Gabor filter. Among them, the orientation is the most important variable in the Gabor filter [16, 37]. Accurate orientation field (OF) estimation of fingerprint image is essential preprocessing step for the Gabor filter. With correct OF of the fingerprint, then we could pick the suitable Gabor filter (same orientation) from the Gabor filter bank (refer to Fig 1.2) which consists of multiple Gabor filters with different orientations and spatial frequencies. By convoluting the fingerprint image with the suitable Gabor filter, we could get a enhanced fingerprint image which strength the features, ridge and valley, of the fingerprint. However, incorrect fingerprint OF estimation can lead to significant distortions in the fingerprint image (refer to Fig 1.3). This is especially true when the estimated orientation is perpendicular to the actual fingerprint orientation [15]. Therefore, it is crucial to prevent poor estimation of the fingerprint OF to ensure accurate fingerprint image enhancing results [13].

Over the past few decades, several methods have been proposed for estimating the orientation field of fingerprint images. These methods include gradient-based techniques [5, 21], slit-based methods [30], frequency domain-based estimations [12, 31], learning-

doi:10.6342/NTU202302201

based models [10, 32], and grayscale intensity variance methods [9, 13, 37]. Among these, the gradient-based approach is the most widely used method for OF estimation because of its high resolution, accuracy, and low computational complexity [6, 7, 15, 20, 22, 27, 34, 36–39]. However, the gradient-based method is sensitive to image quality and may fail to accurately estimate the OF in low-quality fingerprint images [14, 38]. In such cases, other OF estimation methods, such as the frequency domain-based approach, may be more suitable. Some researchers claimed that frequency domain-based OF estimation methods, such as the PSD-based approach, can provide more accurate OF estimation in low-quality fingerprint images. However, these methods are computationally more demanding than the gradient-based. Learning-based models, such as deep neural networks, have also been proposed for OF estimation in fingerprint images. These methods have shown promising results, but they require large amounts of training data and may not be suitable for low-resource environments.

In this study, we propose an alternative method to address the limitations of the gradient-based method for estimating orientation field in low-quality fingerprint images. Our approach is based on differential values of grayscale intensity and involves only convolution calculations to obtain the fingerprint OF estimation field. We demonstrate that our proposed method is more accurate and reliable than both the classic gradient-based estimation and another commonly used OF estimation method, the PSD-based estimation, in the fingerprint images with the Gaussian blurring and the Gaussian white noise. Our experimental results support the effectiveness of our proposed method in improving the accuracy and robustness of OF estimation for low-quality fingerprint images. Overall, our proposed method offers a promising alternative to the classic gradient-based and the PSD-based methods in low quality fingerprint images.

doi:10.6342/NTU202302201

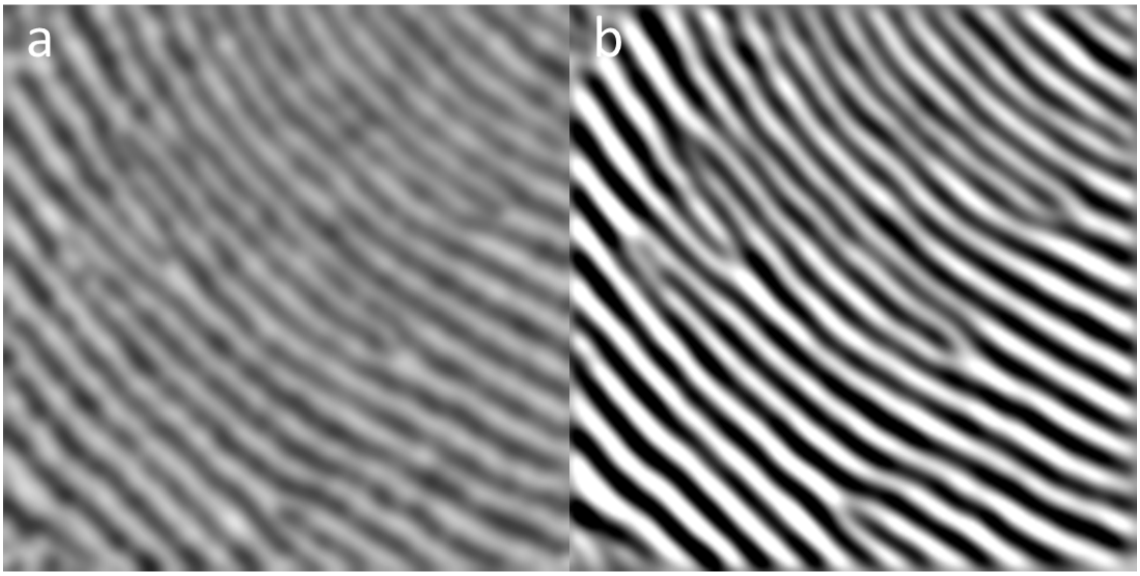

Figure 1.1: Fingerprint image and fingerprint image enhancement with the Gabor filter. (a) Original fingerprint image; (b) Fingerprint image enhancement with the Gabor filter

doi:10.6342/NTU202302201

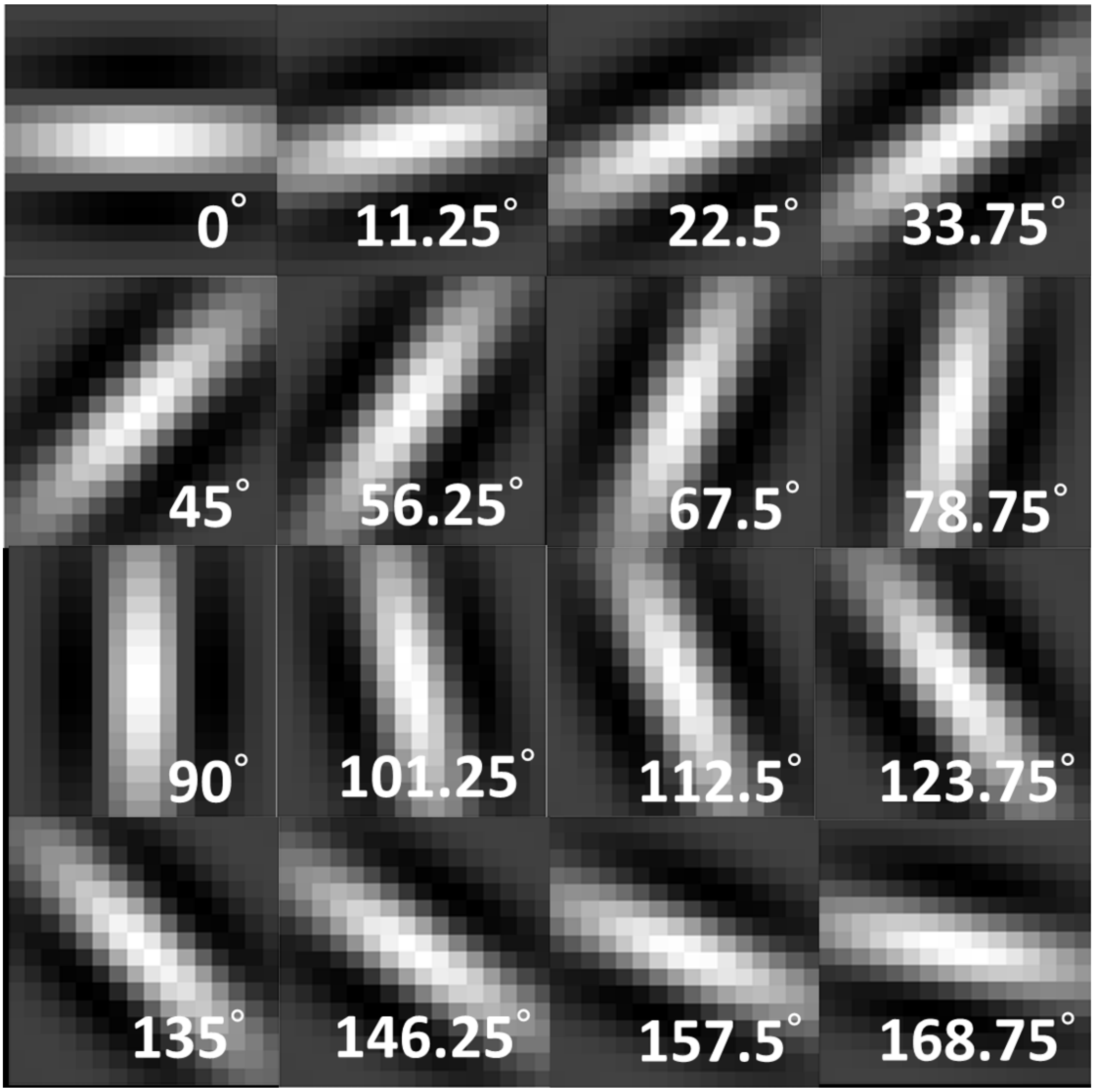

Figure 1.2: Gabor filter bank.

doi:10.6342/NTU202302201

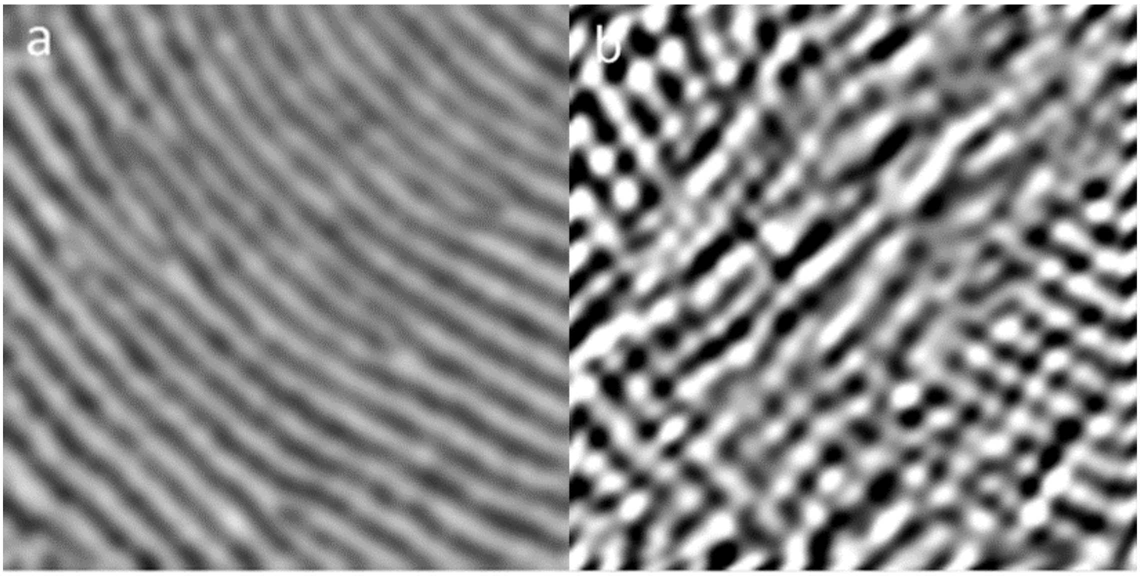

Figure 1.3: Fingerprint image and fingerprint image distortions with the Gabor filter. (a) Original fingerprint image; (b) Fingerprint image distortions with the Gabor filter (wrong orientation)

doi:10.6342/NTU202302201

1.2 Related methods

1.2.1 The gradient-based method

In the gradient-based methods for fingerprint orientation field estimation, the gradient vectors are computed by using the classic Prewitt or Sobel convolution kernels at each pixel, denoted as (G_x, G_y) in Cartesian coordinates. These gradient vectors indicate the directions of the highest variation of grayscale intensity, which are perpendicular to the edges of the ridge lines in the fingerprint image.

The averaged gradient angle computed from the local gradient vectors in a block is denoted as $\overline{\phi}$, and the dominant orientation angle θ is orthogonal to $\overline{\phi}$. However, a ridge line has two edges, and the gradient vectors at both sides of the ridge may be opposite to each other, leading to cancellation during direct averaging of the gradient angles. To overcome this issue, the gradient angles should be doubled before averaging, effectively transforming ϕ into 2ϕ and $(\phi + \pi)$ into $(2\phi + 2\pi)$, which is equivalent to 2ϕ. In practical terms, 2ϕ can be represented as the angle of a squared gradient vector (G_{sx}, G_{sy}), which has a specific relationship with (G_x, G_y) according to trigonometric identities.

$$\begin{bmatrix} G_{sx} \\ G_{sy} \end{bmatrix} = \begin{bmatrix} G^2 \cos 2\phi \\ G^2 \sin 2\phi \end{bmatrix} = \begin{bmatrix} G^2 \left(\cos^2 \phi - \sin^2 \phi\right) \\ G^2 (2 \sin \phi \cos \phi) \end{bmatrix} = \begin{bmatrix} G_x^2 - G_y^2 \\ 2G_x G_y \end{bmatrix} \tag{1.1}$$

The averaged square gradients $(\overline{G}_{sx}, \overline{G}_{sy})$ in a block B can be therefore calculated by:

doi:10.6342/NTU202302201

$$
\begin{bmatrix} \overline{G}_{sx} \\ \overline{G}_{sy} \end{bmatrix} = \begin{bmatrix} \sum_B G_{sx}/N \\ \sum_B G_{sy}/N \end{bmatrix} = \begin{bmatrix} \sum_B \left(G_x^2 - G_y^2\right)/N \\ \sum_B 2G_xG_y/N \end{bmatrix} \tag{1.2}
$$

The direction of orientation field for the block B, θ_B,that is perpendicular to the gradient direction is given by:

$$
\begin{aligned}
\theta_B &= \frac{1}{2}\angle\left(\overline{G}_{sx}, \overline{G}_{sy}\right) + \frac{\pi}{2} \\
&= \frac{1}{2}(2\overline{\phi}) + \frac{\pi}{2} \\
&= \overline{\phi} + \frac{\pi}{2}
\end{aligned} \tag{1.3}
$$

1.2.2 The PSD-based method

The use of 2D Fast Fourier Transform (2D FFT) in fingerprint image analysis is supported by the observation that clear fingerprints display a periodic stripe pattern. This pattern arises from the ridge and valley structures of the fingerprint, resulting in alternating black and white regions in a consistent and repetitive manner. When analyzing a fingerprint image with a unidirectional structure, where fingerprint ridges have a constant width and distance between them, distinctive sharp peaks appear in the Fourier-transformed image, known as power spectrum density (PSD), with the center of the coordinate system as the center of symmetry (see Fig 1.4).

The PSD image generated from the 2D FFT of the fingerprint provides valuable information about the spatial frequency and orientation of the fingerprint ridges. The distance of these sharp peaks from the center of the PSD image indicates the spatial frequency, which relates to the width of the fingerprint ridges. Higher spatial frequencies indicate

doi:10.6342/NTU202302201

narrower ridges, while lower spatial frequencies indicate wider ridges. Additionally, the orientation of the peaks in the PSD image is orthogonal to the orientation of the fingerprint ridges.

doi:10.6342/NTU202302201

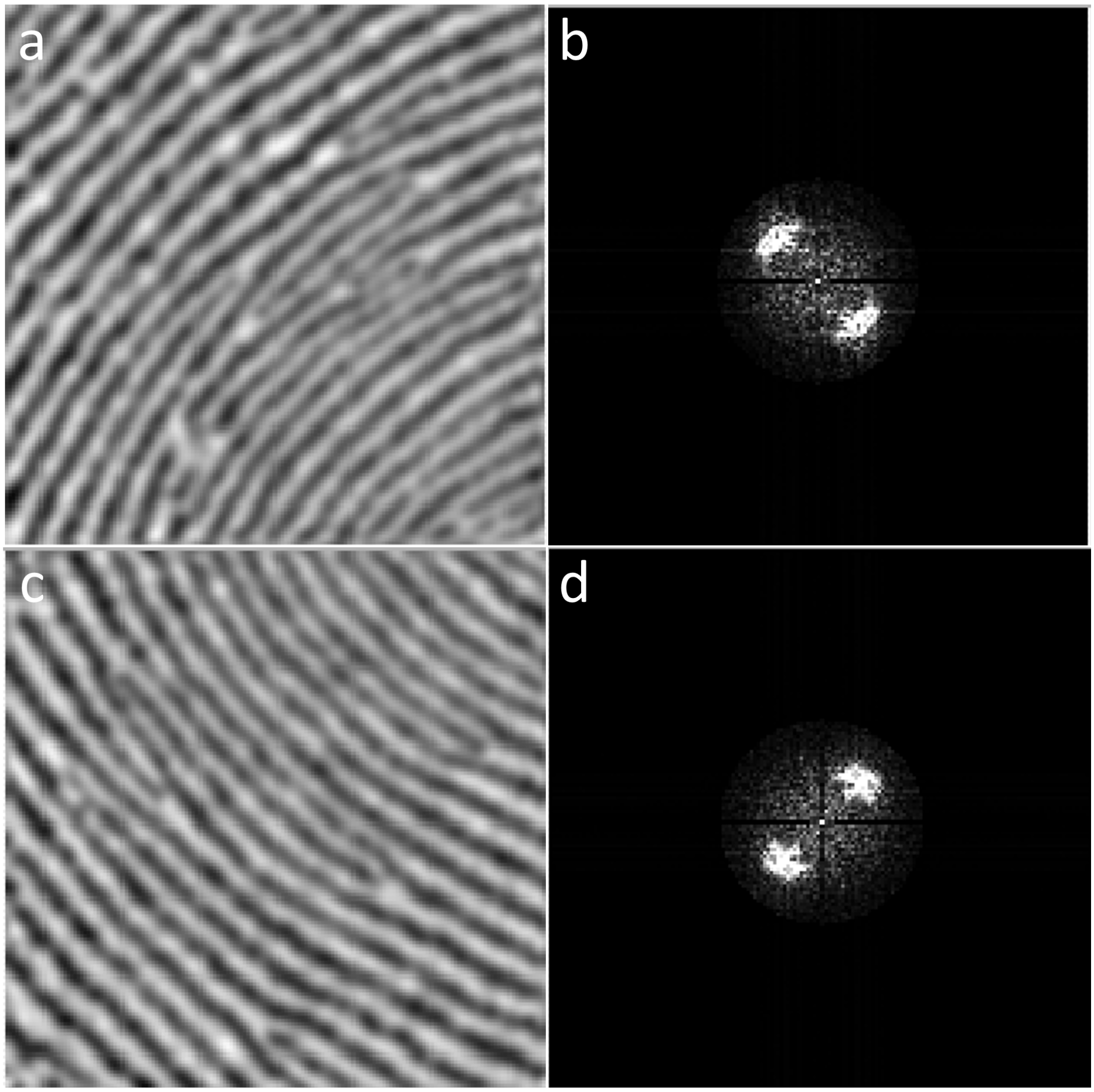

Figure 1.4: Fingerprint images and power spectrum density of fingerprint images. (a) The fingerprint image-a; (b) The PSD of fingerprint image-a; (c) The fingerprint image-b; (d) The PSD of fingerprint image-b

doi:10.6342/NTU202302201

doi:10.6342/NTU202302201

Chapter 2 Methodology

2.1 Differential values of grayscale intensity in each orientation

Fingerprint recognition is a highly effective technology used in various identification and security systems. To extract meaningful information from low quality fingerprint images, improving the quality of fingerprint images is a necessary step and fingerprint enhancement, the Gabor filter, are often employed. It is essential to estimate the orientation field of the fingerprint image for the using of the Gabor filter. In this study, we propose an efficient algorithm for OF estimation using a simple concept based on drawing straight lines through the center of the fingerprint image in different orientations.

We start by drawing N straight lines through the center of the image, where N denoted as the number of orientations. For instance, we use 16 orientations for the fingerprint image in Figure 2.1. When the straight lines are orthogonal to the orientation of the fingerprint, the grayscale intensities are more sensitive along the orientation of the lines. In contrast, if the straight lines are closer to the orientation of fingerprint, the grayscale intensity is less sensitive to changes. We plot the grayscale intensities of the image along each straight line, resulting in a set of line graphs as shown in Figure 2.2. The x-axis represents

doi:10.6342/NTU202302201

the index of each pixel, and the y-axis denoted as the corresponding grayscale intensity of the pixel.

Next, we compute the value of variances in the grayscale intensity for each orientation by differentiating the grayscale intensities of each line and taking its sum of absolute values. Smaller values indicate that the orientation of the straight line is closer to the orientation of the fingerprint. Based on the smaller variances in grayscale intensities, we estimate that the orientation of the fingerprint image in Figure 2.2 is approximately 56.25°.

To simplify the calculations, we substitute differential operations with convolution calculations. In our experimental results, we observe that the performance of the proposed OF estimation algorithm increases with the number of orientations. However, the computational demand of 32 orientations is much higher than that of 16 orientations since the convolution kernel size should increase with the number of orientations. Moreover, the convolution kernel size should not be larger than the pixels between fingerprint ridges width (about 7 pixels in our fingerprint samples) to ensure image convolution could calculate the differential of the grayscale intensities between ridge and valley of fingerprint. Therefore, we select 16 orientations for this study to strike a balance between computational efficiency and accuracy. The number of orientations can be adjusted to trade off between computational complexity and estimation accuracy. The proposed OF estimation process is illustrated in Figure 2.3.

doi:10.6342/NTU202302201

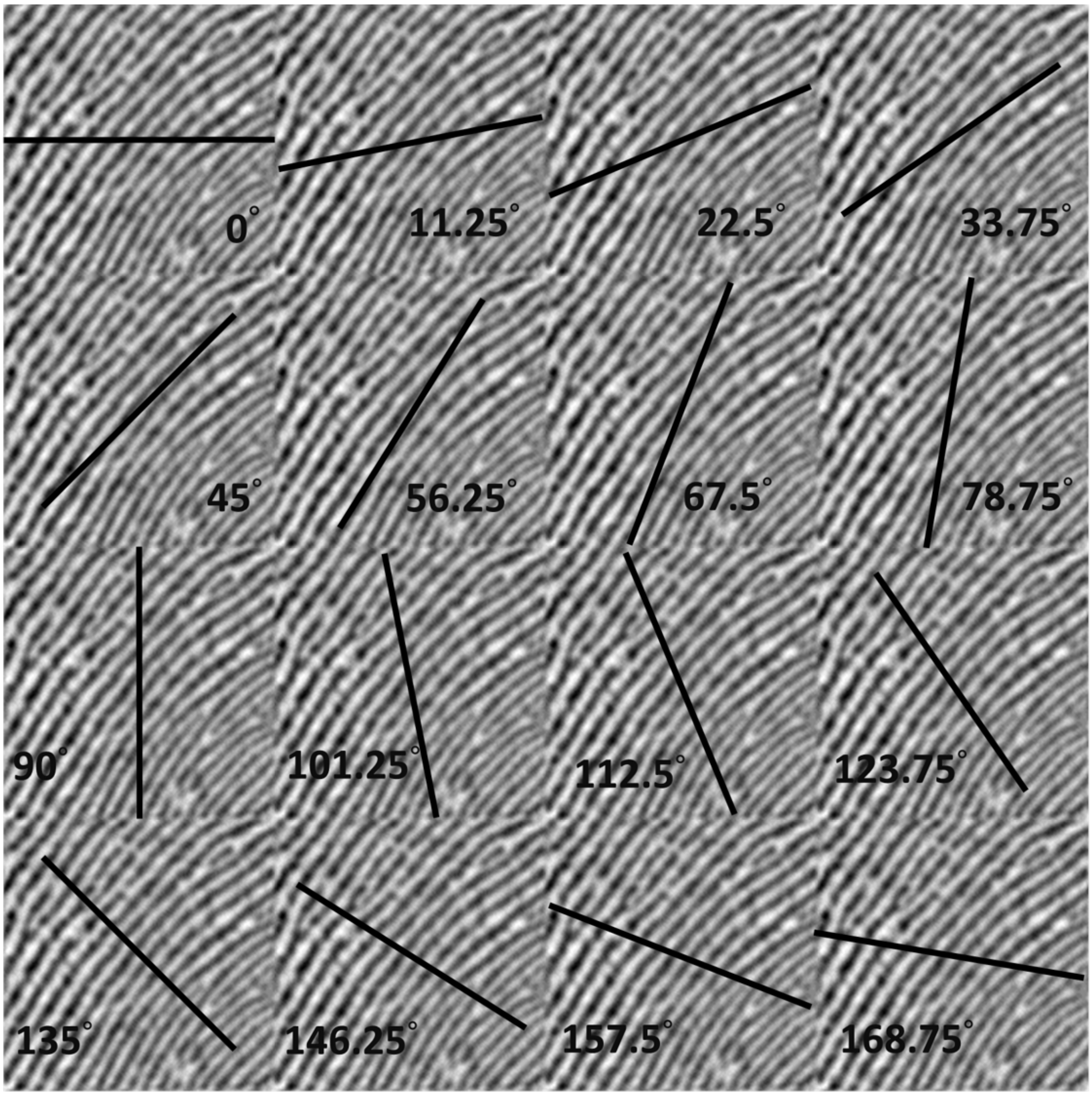

Figure 2.1: Schematic view of 16 orientations of a fingerprint image.

doi:10.6342/NTU202302201

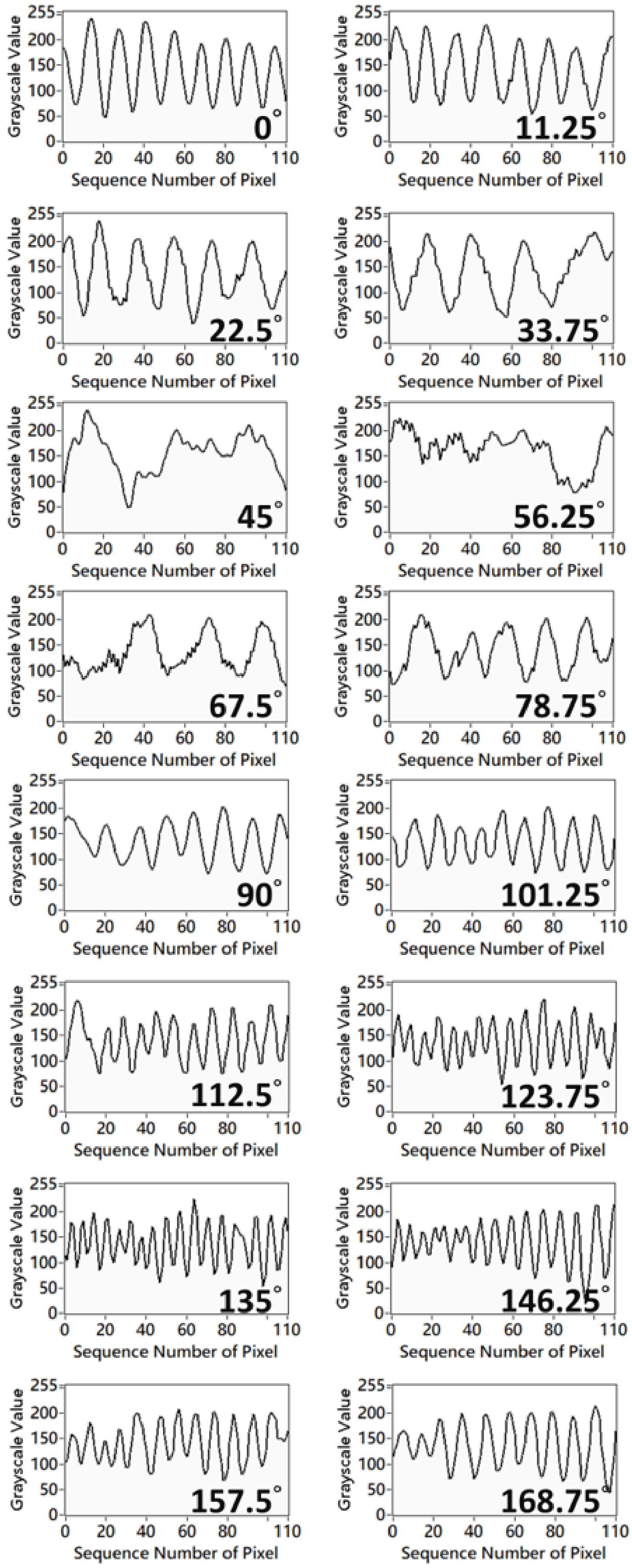

Figure 2.2: Line graphs of grayscale intensities of straight lines in the 16 orientations shown in Figure 2.1.

doi:10.6342/NTU202302201

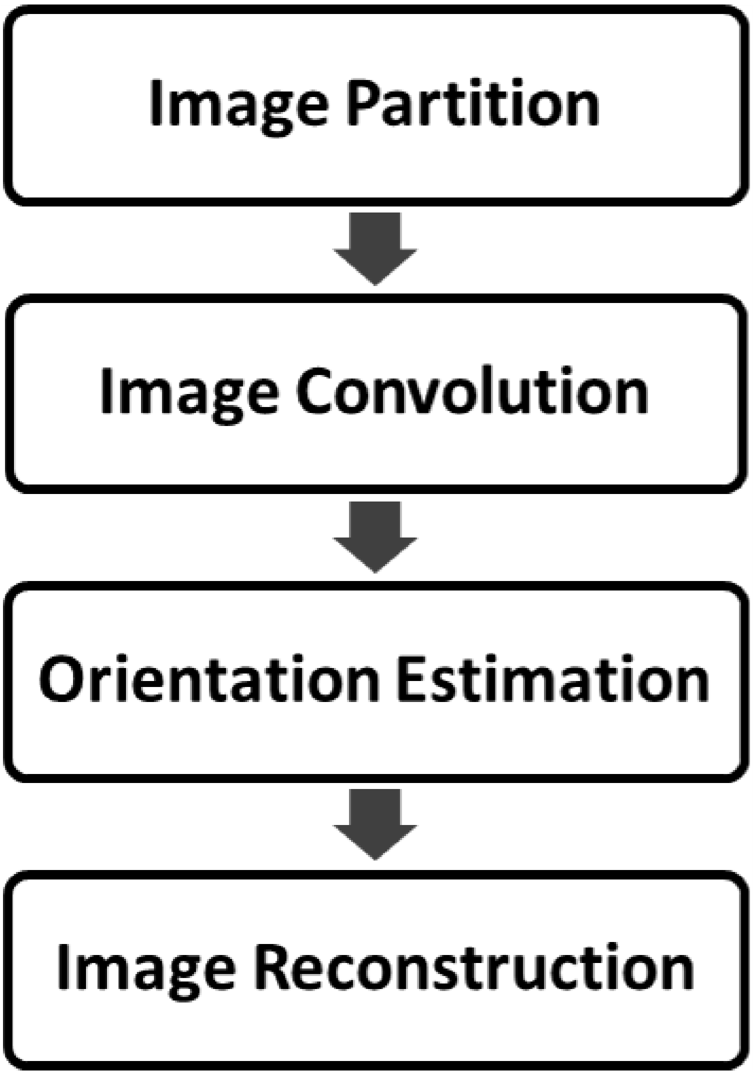

Figure 2.3: The proposed OF estimation process.

doi:10.6342/NTU202302201

2.2 Image partition

The first step of our proposed algorithm involves dividing each fingerprint image into 10 equal parts along both the *x* and *y* axes, resulting in 100 blocks of 16 x 16 pixels per image. The reason why we divide fingerprint image into 100 blocks of 16 x 16 pixels is that we must ensure that blocks size is larger than the gap between the ridge of the fingerprint (the gap is about 7 pixels) and contains a complete ridge and valley of the fingerprint at least. The schematic view of fingerprint image partition is shown in Figure 2.4.

doi:10.6342/NTU202302201

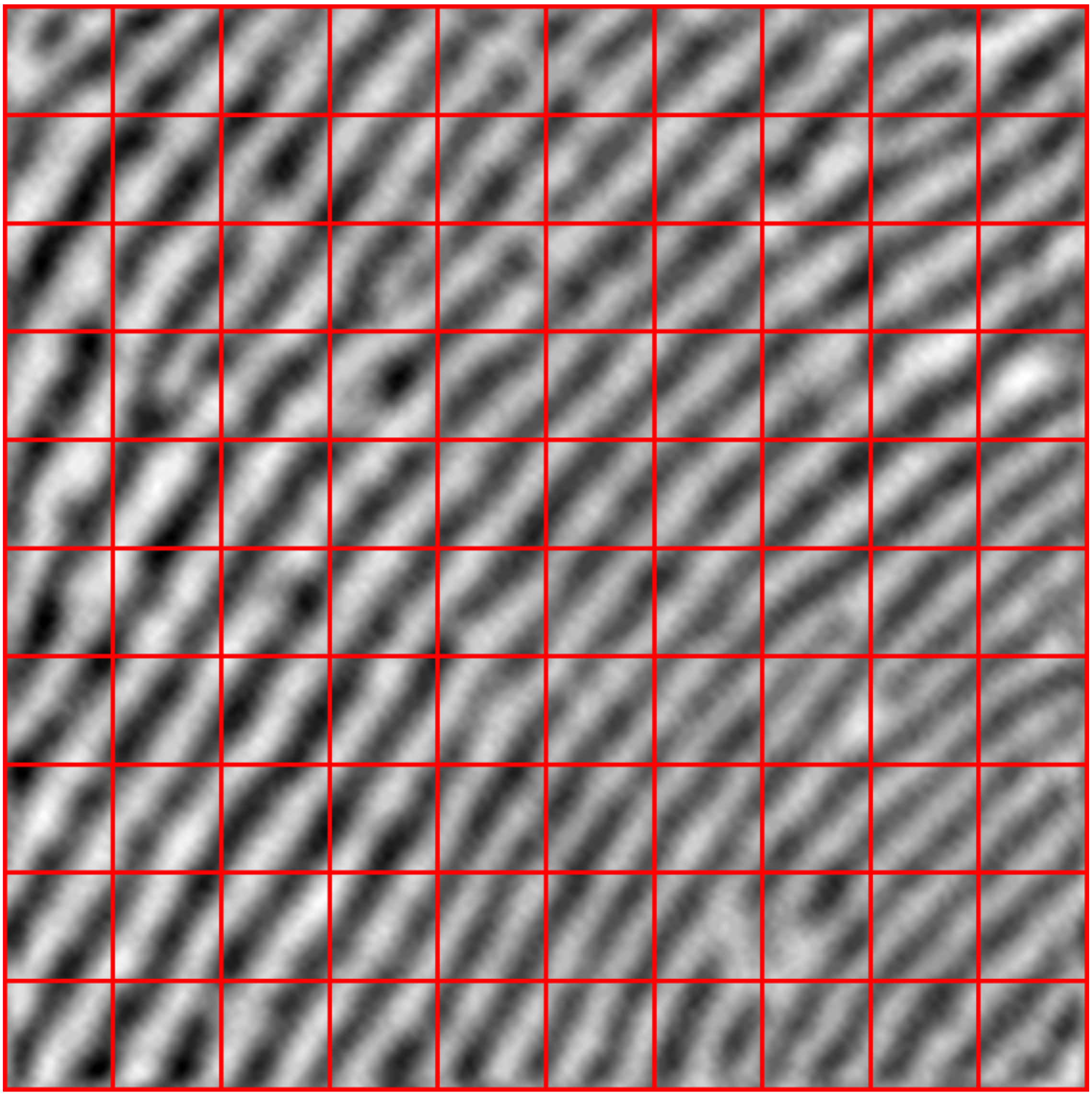

Figure 2.4: Schematic view of fingerprint image partition.

doi:10.6342/NTU202302201

2.3 Image convolution

The second step of the proposed algorithm for estimating the orientation field of fingerprint images involves performing a convolution calculation on each of the 100 blocks obtained from the first step. Equation 2.1 describes the convolution calculation used, where g represents the grayscale intensity of the image, k is the convolution kernel, f is the convolution result, and m, n denoted as the center pixel to perform convolution and i and j denoted as the corresponding pixels covered in the kernel. M, N denoted as the size of fingerprint image, and I, J denoted as the size of kernel. Figure 2.5 shows a example of image convolution process. To perform the convolution calculation, 16 kernels of 5 x 5 are used, with each kernel representing a different orientation. These orientations have an angular difference of 11.25 degrees, which is consistent with the common Gabor filter bank[26, 28]. The result of the convolution calculation is related to the differential grayscale intensity in each orientation. Figure 2.6 shows the convolution kernels of the 16 orientations. For a 2D function $f(x,y)$, the partial differential equation is described in Equation 2.2. However, for discrete data, we can approximate this equation using finite differences, as shown in Equation 2.3. Then, we discuss the Prewitt filter, which comprises two convolution kernels of size 3 x 3 each, as shown in Figure 2.7. These kernels are specifically designed to detect horizontal and vertical edges and can be applied independently to determine the gradient component in each orientation (as G_x and G_y). This is equivalent to the partial differential results for 2D images (Equation 2.3). Therefore, we could utilize this concept to calculate the differential using convolution in our proposed algorithm.

doi:10.6342/NTU202302201

$$\begin{aligned} f[m,n] &= g[m,n] * k[m,n] \\ &= \sum_J \sum_I g[i,j] \cdot k[i-m, j-n] \end{aligned} \tag{2.1}$$

$$\begin{aligned} \frac{\partial f(x,y)}{\partial x} &= \lim_{\varepsilon \to 0} \frac{f(x+\varepsilon, y) - f(x,y)}{\varepsilon} \\ \frac{\partial f(x,y)}{\partial y} &= \lim_{\varepsilon \to 0} \frac{f(x, y+\varepsilon) - f(x,y)}{\varepsilon} \end{aligned} \tag{2.2}$$

$$\begin{aligned} \frac{\partial f(x,y)}{\partial x} &= G_x \approx \frac{f(x+1, y) - f(x,y)}{1} \\ \frac{\partial f(x,y)}{\partial y} &= G_y \approx \frac{f(x, y+1) - f(x,y)}{1} \end{aligned} \tag{2.3}$$

doi:10.6342/NTU202302201

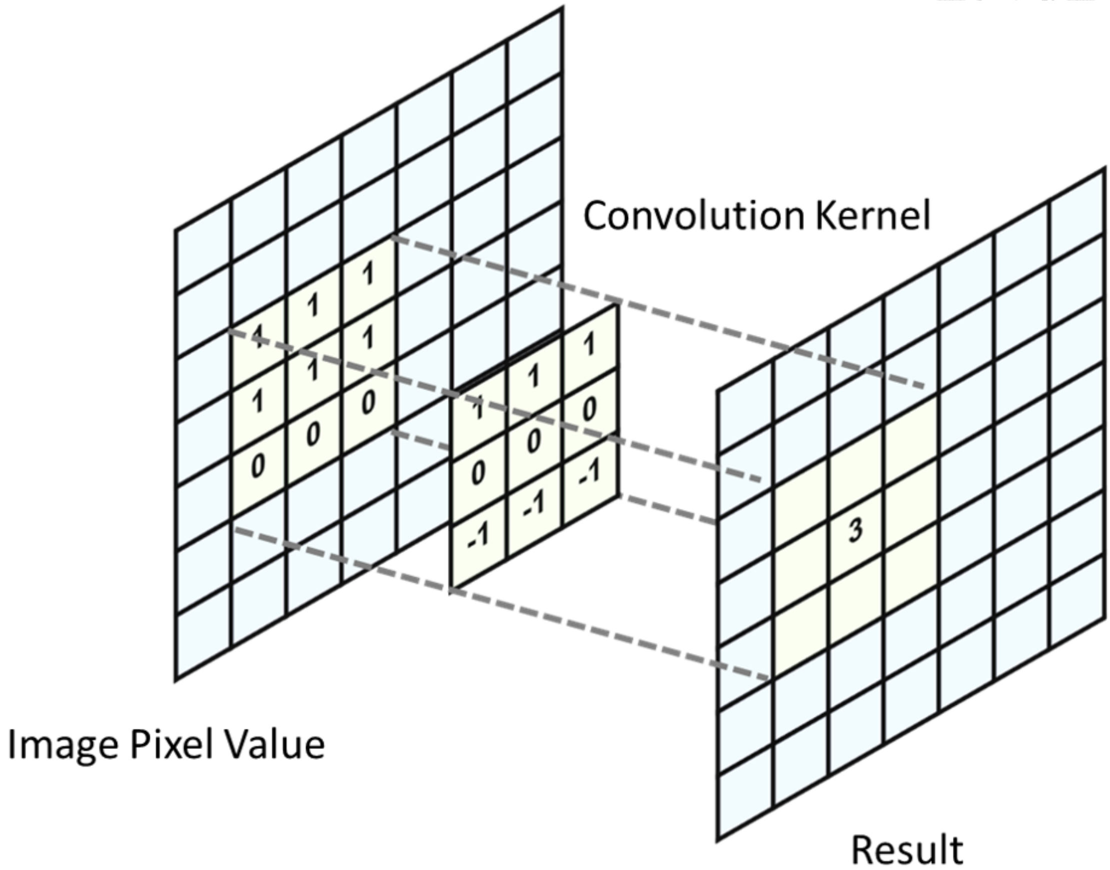

$$
\begin{aligned}
f[2,3] =& \sum_{j}\sum_{i} g[i,j]\cdot h[i-2,j-3] \\
=& g[1,2]\cdot h[-1,-1] + g[2,2]\cdot h[0,-1] + g[3,2]\cdot h[1,-1] \\
& + g[1,3]\cdot h[-1,0] + g[2,3]\cdot h[0,0] + g[3,3]\cdot h[1,0] \\
& + g[1,4]\cdot h[-1,1] + g[2,4]\cdot h[0,1] + g[3,4]\cdot h[1,1] \\
=& 1\cdot 1 + 1\cdot 1 + 1\cdot 1 \\
& + 0\cdot 1 + 0\cdot 1 + 0\cdot 1 \\
& + (-1)\cdot 0 + (-1)\cdot 0 + (-1)\cdot 0 \\
=& 3
\end{aligned}
$$

Figure 2.5: A example of image convolution process.

doi:10.6342/NTU202302201

$$\begin{bmatrix} 0&0&0&0&0\\ 0&0&0&0&0\\ -1&0&0&0&+1\\ 0&0&0&0&0\\ 0&0&0&0&0 \end{bmatrix}$$

0°

$$\begin{bmatrix} 0&0&0&0&0\\ 0&0&0&0&+1\\ -1&0&0&0&0\\ 0&0&0&0&0\\ 0&0&0&0&0 \end{bmatrix}$$

11.25°

$$\begin{bmatrix} 0&0&0&0&0\\ 0&0&0&0&+1\\ 0&0&0&0&0\\ -1&0&0&0&0\\ 0&0&0&0&0 \end{bmatrix}$$

22.5°

$$\begin{bmatrix} 0&0&0&0&+1\\ 0&0&0&0&0\\ 0&0&0&0&0\\ -1&0&0&0&0\\ 0&0&0&0&0 \end{bmatrix}$$

33.75°

$$\begin{bmatrix} 0&0&0&0&+1\\ 0&0&0&0&0\\ 0&0&0&0&0\\ 0&0&0&0&0\\ -1&0&0&0&0 \end{bmatrix}$$

45°

$$\begin{bmatrix} 0&0&0&+1&0\\ 0&0&0&0&0\\ 0&0&0&0&0\\ 0&0&0&0&0\\ -1&0&0&0&0 \end{bmatrix}$$

56.25°

$$\begin{bmatrix} 0&0&0&+1&0\\ 0&0&0&0&0\\ 0&0&0&0&0\\ 0&0&0&0&0\\ 0&-1&0&0&0 \end{bmatrix}$$

67.5°

$$\begin{bmatrix} 0&0&+1&0&0\\ 0&0&0&0&0\\ 0&0&0&0&0\\ 0&0&0&0&0\\ 0&-1&0&0&0 \end{bmatrix}$$

78.75°

$$\begin{bmatrix} 0&0&+1&0&0\\ 0&0&0&0&0\\ 0&0&0&0&0\\ 0&0&0&0&0\\ 0&0&-1&0&0 \end{bmatrix}$$

90°

$$\begin{bmatrix} 0&+1&0&0&0\\ 0&0&0&0&0\\ 0&0&0&0&0\\ 0&0&0&0&0\\ 0&0&-1&0&0 \end{bmatrix}$$

101.25°

$$\begin{bmatrix} 0&+1&0&0&0\\ 0&0&0&0&0\\ 0&0&0&0&0\\ 0&0&0&0&0\\ 0&0&0&-1&0 \end{bmatrix}$$

112.5°

$$\begin{bmatrix} +1&0&0&0&0\\ 0&0&0&0&0\\ 0&0&0&0&0\\ 0&0&0&0&0\\ 0&0&0&-1&0 \end{bmatrix}$$

123.75°

$$\begin{bmatrix} +1&0&0&0&0\\ 0&0&0&0&0\\ 0&0&0&0&0\\ 0&0&0&0&0\\ 0&0&0&0&-1 \end{bmatrix}$$

135°

$$\begin{bmatrix} 0&0&0&0&0\\ +1&0&0&0&0\\ 0&0&0&0&0\\ 0&0&0&0&0\\ 0&0&0&0&-1 \end{bmatrix}$$

146.25°

$$\begin{bmatrix} 0&0&0&0&0\\ +1&0&0&0&0\\ 0&0&0&0&0\\ 0&0&0&0&-1\\ 0&0&0&0&0 \end{bmatrix}$$

157.5°

$$\begin{bmatrix} 0&0&0&0&0\\ 0&0&0&0&0\\ +1&0&0&0&0\\ 0&0&0&0&-1\\ 0&0&0&0&0 \end{bmatrix}$$

168.75°

Figure 2.6: The convolution kernels of the 16 orientations.

doi:10.6342/NTU202302201

−1	0	+1
−1	0	+1
−1	0	+1

a

+1	+1	+1
0	0	0
−1	−1	−1

b

Figure 2.7: The Prewitt filter kernels. (a) Kernel of G_x; (b) Kernel of G_y

doi:10.6342/NTU202302201

2.4 Orientation field estimation (index, matrices)

In the third step of the proposed algorithm for estimating the orientation field of fingerprint images, the sum of the absolute grayscale intensities for each block after convolution is computed. This sum is represented as F for all 16 orientations (kernels). The minimum F value is then determined using Equation 2.4. A higher F value indicates more variances in grayscale intensity in the orientation and more orthogonal orientation relative to the fingerprint orientation. Conversely, a lower F value implies greater parallelism with the fingerprint orientation.

To estimate the orientation field, the two minimum F values are weighted, and their weighted average is computed using Equation 2.5, because we want to improve the accuracy of fingerprint orientation field estimation, rather than being limited to only 16 orientations.

$$\begin{aligned} F &= \sum_{N}\sum_{M} |f[m,n]| \\ F_{\text{min}} &= \text{min}\left(F_1, F_2, F_3, \cdots F_{16}\right) \end{aligned} \tag{2.4}$$

$$OF_{\text{weighted average}} = OF_{\text{min 1}} \times \frac{\frac{1}{F_{\text{min 1}}}}{\frac{1}{F_{\text{min 1}}} + \frac{1}{F_{\text{min 2}}}} + OF_{\text{min 2}} \times \frac{\frac{1}{F_{\text{min 2}}}}{\frac{1}{F_{\text{min 1}}} + \frac{1}{F_{\text{min 2}}}} \tag{2.5}$$

2.5 Image reconstruction

The proposed algorithm entails a fourth step that involves assembling the 100 individual blocks to generate the estimated fingerprint OF for the whole fingerprint image.

doi:10.6342/NTU202302201

This step serves to create a comprehensive representation of the entire fingerprint for further analysis. The resulting OF is illustrated in Figure 2.8, which depicts both the original fingerprint image and the estimated fingerprint OF. The process of image reconstruction is a important aspect of the algorithm as it ensures that the reconstructed image is a faithful representation of the original fingerprint and could verify the accuracy of the orientation field estimation of fingerprints.

doi:10.6342/NTU202302201

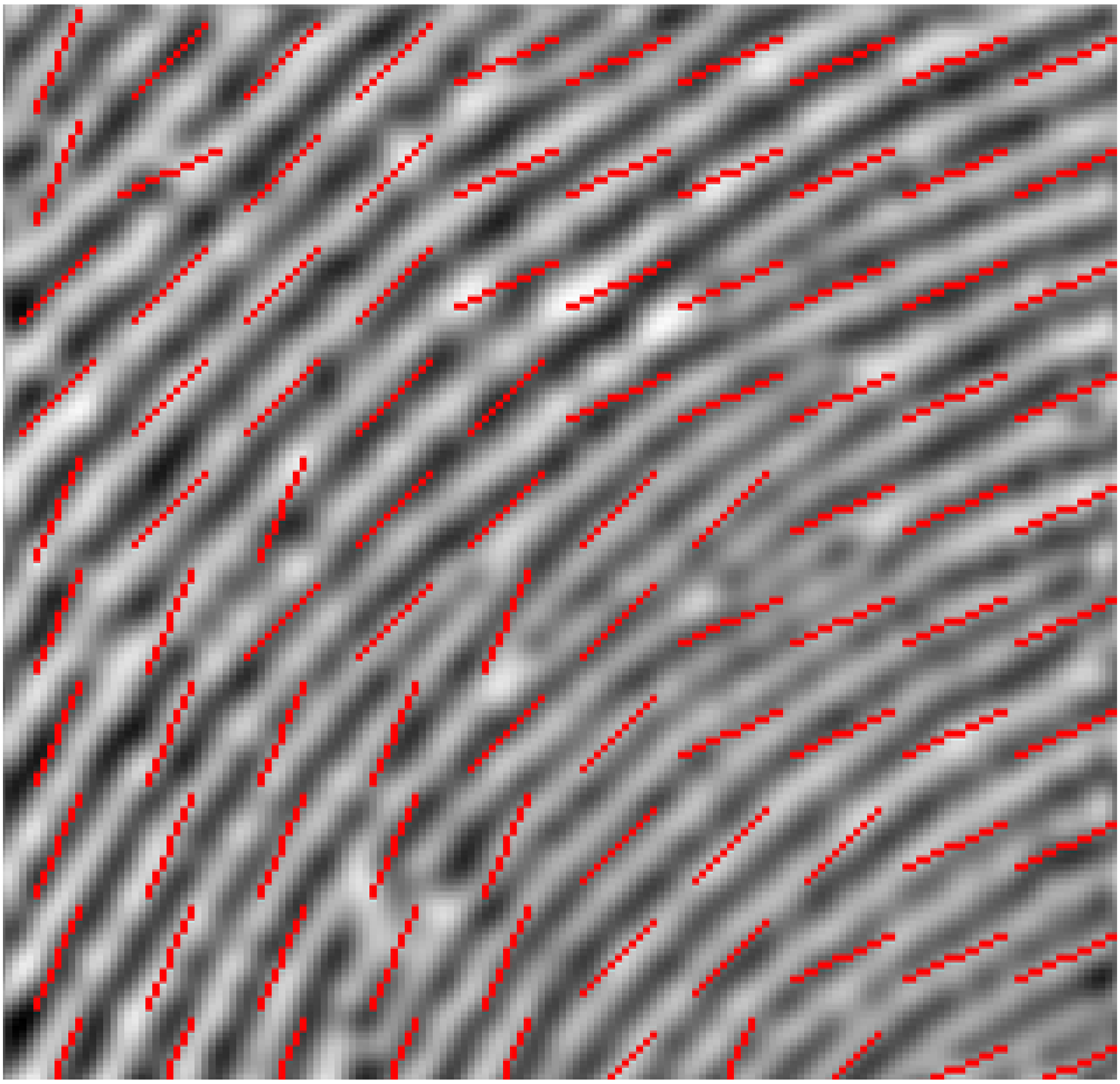

Figure 2.8: Fingerprint image and fingerprint OF.

doi:10.6342/NTU202302201

doi:10.6342/NTU202302201

Chapter 3 Experiments and Results

This study presents three experiments aimed at evaluating the accuracy and reliability of a proposed algorithm for estimating orientation field in fingerprint images. The experiments involve comparing the results of the proposed algorithm with the classic OF gradient-based and the PSD-based methods.

Experiment 1 evaluates the accuracy of the proposed algorithm by selecting 15 clear fingerprint images (as shown in Figure 3.1a), calculating the OF estimations using the proposed algorithm, and comparing the results with the classic gradient-based and the PSD-based methods. The experiment validates that the proposed algorithm produces accurate OF estimations for clear fingerprint images.

Experiment 2 evaluates the accuracy of the proposed algorithm in blurred fingerprint images. The Gaussian blurring is performed on each fingerprint image (as shown in Figure 3.1b), and the OF estimations of the original and blurred fingerprint images are calculated using the proposed algorithm, the gradient-based method, and the PSD-based method. The experiment validates that the proposed algorithm is reliable in estimating OF in blurred fingerprint images.

Experiment 3 evaluates the accuracy of the proposed algorithm in noisy fingerprint images. The Gaussian white noise is added to each fingerprint image (as shown in Figure

doi:10.6342/NTU202302201

3.1c), and the OF estimations of the original and noisy fingerprint images are calculated using the proposed algorithm, the gradient-based method, and the PSD-based method. The experiment validates that the proposed algorithm is reliable in estimating OF in noisy fingerprint images.

we also utilize statistical tool, correlation analysis to validate the accuracy and reliability of our proposed OF estimation algorithm. The correlation coefficient, denoted as ”r”, is a widely used statistical measurement that quantifies the strength and direction of the linear relationship between two variables. It is calculated using statistical methods, such as the Pearson’s correlation coefficient, and is a numerical value that ranges between -1 and 1. A positive correlation coefficient ($r > 0$) indicates a positive linear relationship between the two variables. This means that as one variable increases, the other variable tends to increase as well, and as one variable decreases, the other variable tends to decrease as well. For example, in a study investigating the relationship between age and income, a positive correlation coefficient would suggest that as age increases, income tends to increase as well. On the other hand, a negative correlation coefficient ($r < 0$) indicates a negative linear relationship between the two variables. This means that as one variable increases, the other variable tends to decrease. For example, in a study examining the relationship between temperature and hot coffee, a negative correlation coefficient would suggest that as temperature increases, hot coffee sales tend to decrease. A correlation coefficient of 0 ($r = 0$) indicates no linear relationship between the two variables. This means that changes in one variable are not associated with changes in the other variable. However, it is important to note that even when the correlation coefficient is 0, there may still be other types of relationships between the variables that are not captured by the linear correlation coefficient. The magnitude of the correlation coefficient (i.e., how close it

doi:10.6342/NTU202302201

is to -1 or 1) reflects the strength of the relationship. A correlation coefficient of -1 or 1 indicates a perfect linear relationship, where all data points fall exactly on a straight line.

All the algorithms are developed and implemented in LabVIEW (short for Laboratory Virtual Instrument Engineering Workbench) which is a powerful graphical programming language and development environment used for creating custom applications that control and automate laboratory equipment and processes. Developed by National Instruments in 1986, LabVIEW has become a popular tool in many fields, including engineering, physics, biology, chemistry, and more. The language is based on a dataflow programming model, which means that program execution is determined by the flow of data through a set of interconnected nodes, rather than by explicit program instructions. LabVIEW's unique graphical user interface (GUI) allows users to create programs by dragging and dropping graphical icons representing functions, data structures, and control flow structures. These icons are connected together using wires, which carry data and signals between the different parts of the program. The resulting program, or VI (Virtual Instrument), can be run on a computer or deployed to a variety of hardware platforms, including embedded systems and data acquisition devices.

The LabVIEW VDM (Vision Development Module) is a software module of LabVIEW that helps us develop machine vision algorithm and found to be suitable for our study. Using LabVIEW VDM helps the creation of our proposed fingerprint OF estimation algorithm, because the LabVIEW VDM intuitive user interface and comprehensive library of pre-built machine vision functions also allowed for streamlined development and faster prototyping of algorithms. These are the reasons why we develop our fingerprint OF estimation algorithm with LabVIEW and our source code of the proposed algorithm (partial) and GUI as shown in Figure 3.2.

doi:10.6342/NTU202302201

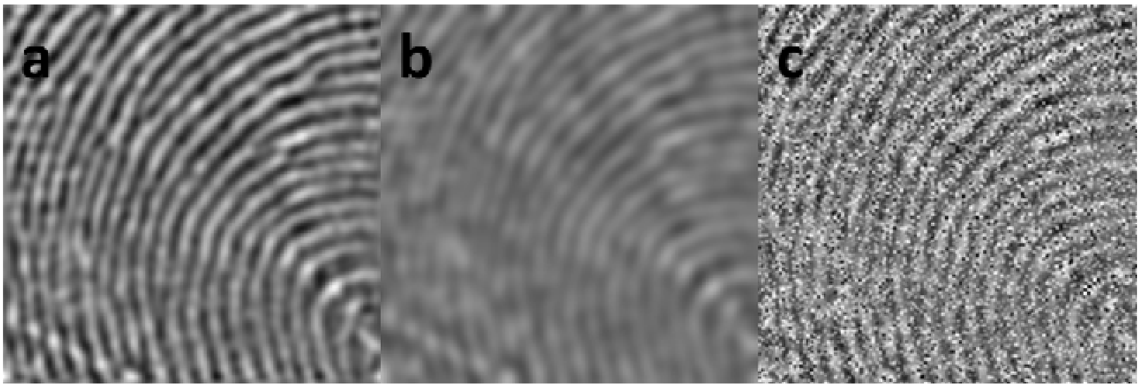

Figure 3.1: Fingerprint image samples for experiments: (a) Original Sample; (b) Blurred Sample; (c) Noisy Sample

doi:10.6342/NTU202302201

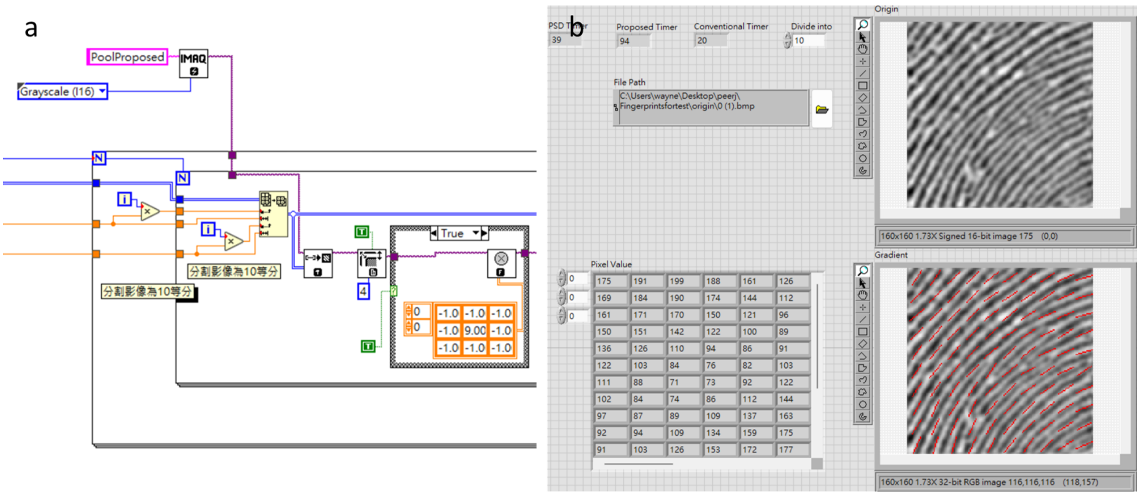

Figure 3.2: LabVIEW source code and GUI: (a) Source code; (b) GUI

doi:10.6342/NTU202302201

3.1 Database

In this study, we use the fingerprint data of volunteers, which are captured with an OLED panel display image sensor. These fingerprint images are only used for orientation field estimation, which is explained to the study participants. No personal information such as age, gender, and name, are collected from the volunteers. The study dataset included 2520 images (126 finger samples, with 20 elements each). The resolution of each sample is 160 × 160 pixels.

3.2 Experiment 1: Accuracy assessment in clear fingerprint images

In this study, we propose a new algorithm for estimating the OF of fingerprints and compare its accuracy to two commonly used methods - the gradient-based method and the PSD-based method. We conducte an experiment using 15 fingerprint images from our study database and compute the OF using the three methods. The results are compared, and we find that our proposed algorithm's OF estimation is similar to that of the gradient-based method, whereas the PSD-based method has more differences with the gradient-based method.

To evaluate the accuracy of the three methods, we compare the deviation of the estimated OF from the actual OF in 1,500 blocks of the 15 fingerprint images. From Figure 3.3, We could find that our proposed algorithm has a deviation of more than 20 degrees in 67 blocks, while the PSD-based method has a deviation of more than 20 degrees in 119 blocks. We considere these deviations as misinterpretations, and we calculate the accu-

doi:10.6342/NTU202302201

racy rate of our proposed algorithm and the PSD-based method. We find that the accuracy rate of our proposed algorithm is 95.53%, which is higher than the 92.06% accuracy rate for the PSD-based method. This indicates that our proposed algorithm is a more reliable and accurate method for estimating the OF of clear fingerprints.

We also analyze the error blocks in the fingerprints and find that they are primarily concentrated around the edges of the fingerprint (as shown in Figure 3.4). This is not surprising, as the edges of the fingerprints tend to have the lowest image quality, which makes it more challenging to obtain accurate data. Furthermore, we find that the core area of the fingerprint, which is a semi-circle or an arc, lacks obvious orientations, making it difficult to define the orientation of the overall fingerprint in those core blocks.

At last, we conducte a correlation coefficient analysis to compare the three methods. We find that our proposed algorithm shows a strong positive correlation (r = 0.909) with the gradient-based method, indicating that the two methods are highly correlated. In comparison, the correlation coefficient between the PSD-based method and the gradient-based method is found to be 0.755, which is lower than the correlation coefficient between the proposed algorithm and the gradient-based method. These findings further support the conclusion that our proposed algorithm is a more reliable and accurate method for estimating the OF of clear fingerprints. From Figure 3.5, OF estimation of each fingerprint block on clear fingerprint images, we could confirm the result about correlation coefficient analysis as well, the trend is close between the the proposed algorithm and the gradient-based method.

doi:10.6342/NTU202302201

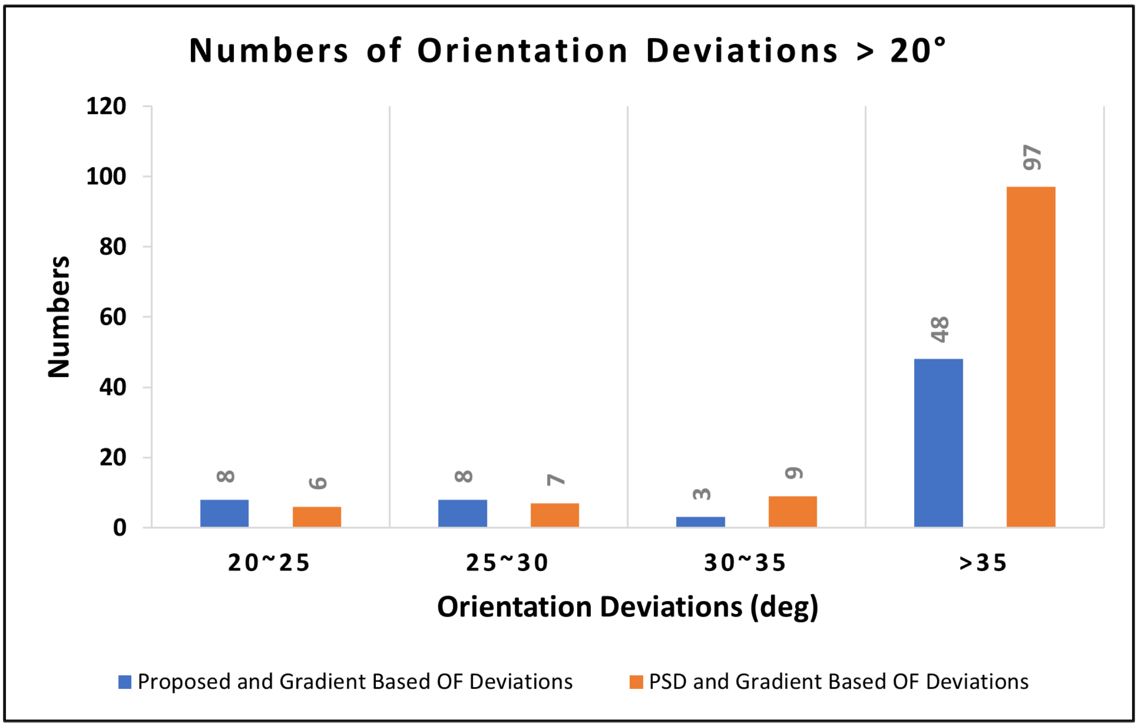

Figure 3.3: Deviations in the estimated OF between the proposed method/the PSD-based method and the gradient-based method on clear fingerprint images (1,500 blocks).

doi:10.6342/NTU202302201

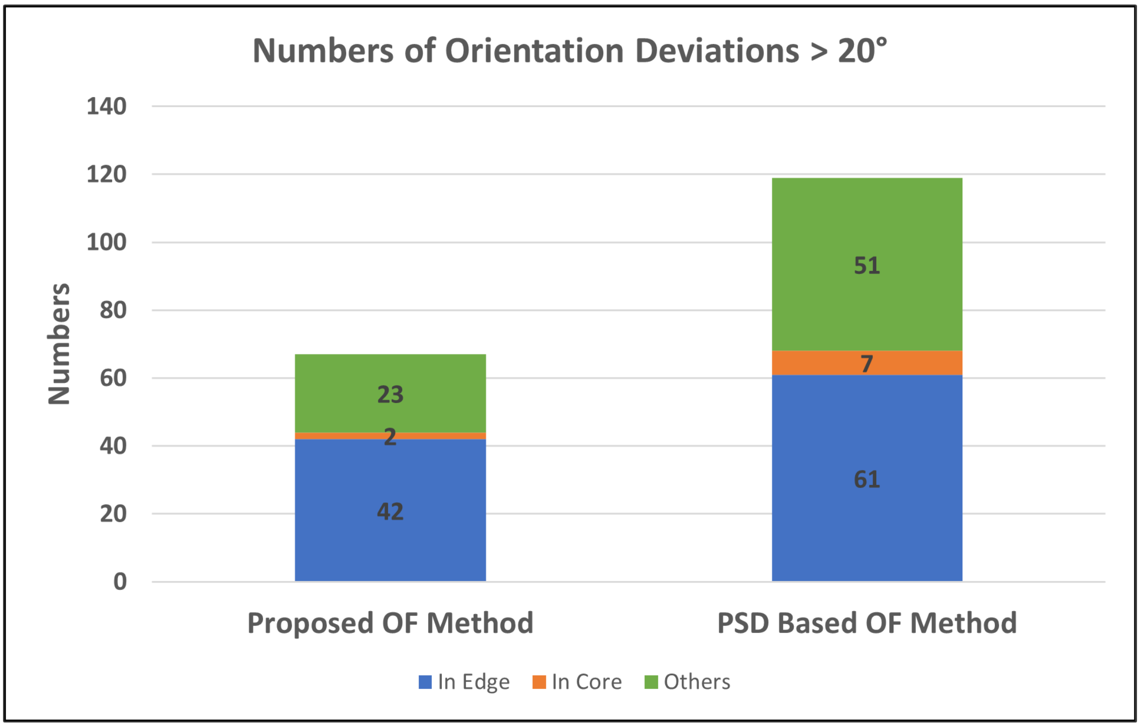

Figure 3.4: Deviations in the estimated OF between the proposed method/the PSD-based method and the gradient-based method on clear fingerprint images (1,500 blocks) by location.

doi:10.6342/NTU202302201

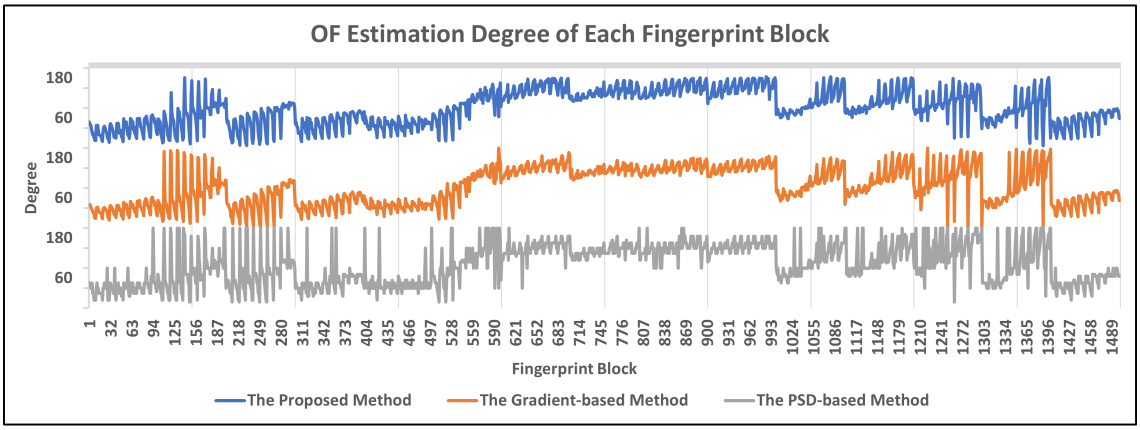

Figure 3.5: OF estimation of each fingerprint block on clear fingerprint images using the proposed method, the gradient-based method and the PSD-based method (1,500 blocks).

doi:10.6342/NTU202302201

3.3 Experiment 2: Accuracy assessment in blurred fingerprint images

The reliability of the proposed OF estimation algorithm on blurred fingerprint images is tested in this study. The Gaussian blurring is applied to 15 fingerprint images selected in Experiment 1 using a 7x7 Gaussian kernel. The proposed algorithm, the gradient-based method, and the PSD-based method are used to calculate the estimated OF of both the original (clear) and blurred fingerprint images. The results are compared to determine the reliability of the proposed algorithm on blurred images. The Gaussian blurring is a nonuniform low-pass filter that blurs the details of an image but preserves low spatial frequencies and reduces image noise. It is achieved by convoluting an image with a 7x7 Gaussian kernel. The 7x7 Gaussian kernel used in this study is shown in Figure 3.6.

The histograms of the results (shown in Figure 3.7) indicate that the estimated OF results of the clear and blurred fingerprint images calculated by the proposed algorithm differs only slightly. The proposed algorithm produces an accuracy rate of 99.53%, with only 7 blocks having an orientation deviation of more than 20 degrees. The average orientation deviation is 1.81°, and the correlation coefficient is 0.995. These results demonstrate the reliability of the proposed algorithm for estimating OF in blurred fingerprint images.

In contrast, the OF estimation results of the gradient-based method for clear and blurred fingerprint images resulted in 13 blocks with an orientation deviation of more than 20 degrees, indicating an accuracy rate of 99.13%. The average orientation deviation is 2.18°, and the correlation coefficient is 0.978. The PSD-based OF estimation results of the clear and blurred fingerprint images result in 126 blocks with an orientation deviation

doi:10.6342/NTU202302201

of more than 20 degrees, an accuracy rate of 91.6%, an average orientation deviation of 6.92°, and the correlation coefficient is 0.868. As shown in Figure 3.8 - 3.10, OF estimation of each fingerprint block on blurred fingerprint images, the correlation coefficient analysis also confirms that the orientation field estimation results in the proposed algorithm and the gradient-based method both show a close trend between clear and blurred fingerprints, however, there is a slight difference observed in the orientation field estimation results between clear and blurring fingerprints in the PSD-based method.

In conclusion, the proposed algorithm shows promising results in estimating OF in blurred fingerprint images. Its accuracy rate is high, and its orientation deviation and correlation coefficient are both good, indicating that it produces reliable and consistent results. This experiment provides evidence that the proposed algorithm can be used in real-world scenarios where fingerprint images may be blurred due to environmental factors or poor image quality. The study's results demonstrate that it outperforms the gradient-based and the PSD-based methods in blurred fingerprint images.

doi:10.6342/NTU202302201

0	0	1	2	1	0	0
0	3	13	22	13	3	0
1	13	59	97	59	13	1
2	22	97	159	97	22	2
1	13	59	97	59	13	1
0	3	13	22	13	3	0
0	0	1	2	1	0	0

Figure 3.6: The Gaussian blurring kernel.

doi:10.6342/NTU202302201

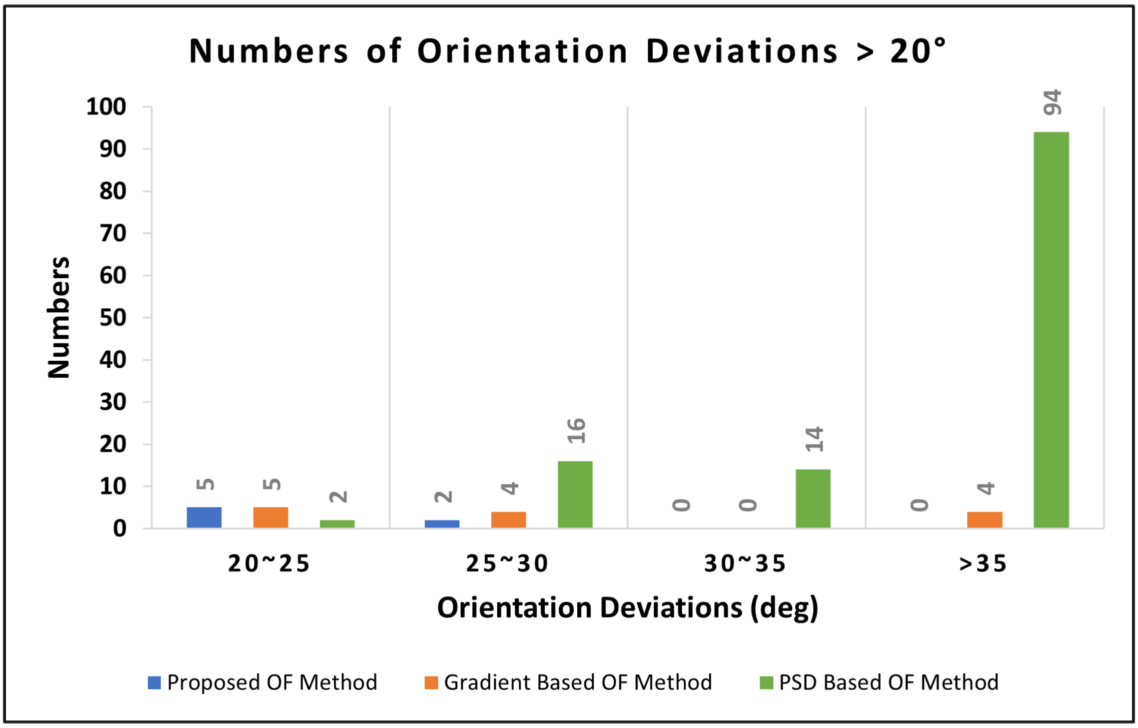

Figure 3.7: Deviations in estimated OF between clear and blurred fingerprint images (1,500 blocks).

doi:10.6342/NTU202302201

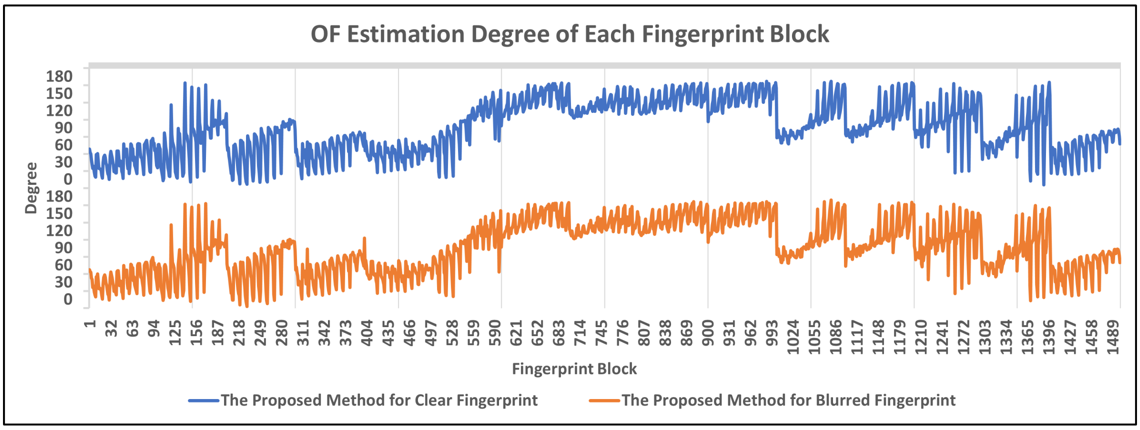

Figure 3.8: OF estimation of each fingerprint block on blurred fingerprint images using the proposed method (1,500 blocks).

doi:10.6342/NTU202302201

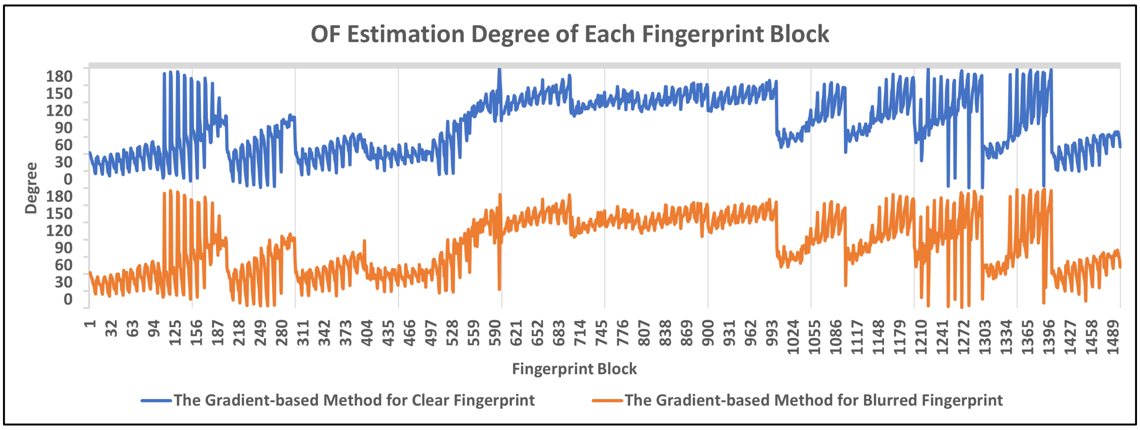

Figure 3.9: OF estimation of each fingerprint block on blurred fingerprint images using the gradient-based method (1,500 blocks).

doi:10.6342/NTU202302201

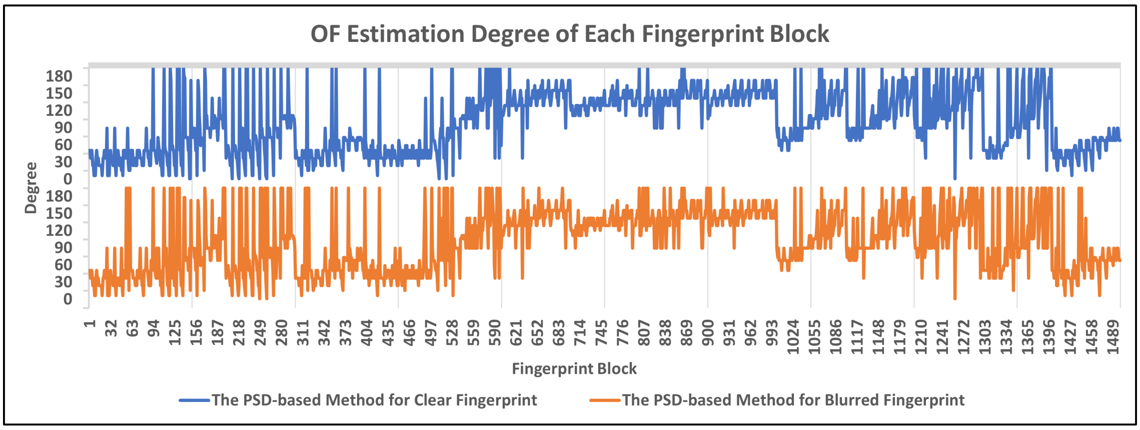

Figure 3.10: OF estimation of each fingerprint block on blurred fingerprint images using the PSD-based method (1,500 blocks).

doi:10.6342/NTU202302201

3.4 Experiment 3: Accuracy assessment in noisy fingerprint images

To assess the reliability of the proposed OF estimation algorithm in noisy fingerprint images, an experiment is conducted on 15 selected fingerprint images. The Gaussian white noise process, a technique used to add random noise values from a the Gaussian distribution to an image, is applied to these 15 fingerprint images. Then we estimate the OF of the original (clear) and noisy images using the proposed algorithm, the gradient-based method, and the PSD-based method. The purpose of the experiment is to compare the results of all three methods and determine the reliability of the proposed algorithm in noisy fingerprint images.

The results of the experiment, displayed in Figure 3.11, show that the estimated OF results of clear and noisy fingerprint images differ significantly more than the blurred fingerprints in Experiment 2 for all three algorithms. However, the proposed algorithm outperforms the gradient-based and the PSD-based methods in OF estimation in noisy fingerprint images. The proposed algorithm has 383 blocks with an orientation deviation of over 20 degrees, giving it an accuracy rate of 74.46%, an average orientation deviation of 13.86°, and a correlation coefficient of 0.898. The gradient-based method produces 480 blocks with an orientation deviation of more than 20 degrees, resulting in an accuracy rate of 68%, an average orientation deviation of 21.79°, and a correlation coefficient of 0.661. The PSD-based method produces 877 blocks with an orientation deviation of more than 20 degrees, an accuracy rate of 41.53%, an average orientation deviation of 42.19°, and a correlation coefficient of 0.236. The observation from Figure 3.12 - 3.14, which displays the orientation field estimation of each fingerprint block on the clear and noisy

doi:10.6342/NTU202302201

fingerprint images, reveals that the trends in the clear and noisy fingerprints orientation field estimation diverge significantly in all three algorithms. However, it is evident that the difference between the results of clear and noisy fingerprints orientation field estimation in the proposed algorithm is notably smaller compared to the other methods.

In conclusion, the experiment shows that the proposed algorithm is reliable for estimating OF in noisy fingerprint images. The proposed algorithm outperforms the gradient-based and the PSD-based methods in OF estimation in noisy fingerprint images. Table 1 and Table 2 compare the performance and positive/negative aspects of the proposed algorithm and the two classic OF estimation methods.

doi:10.6342/NTU202302201

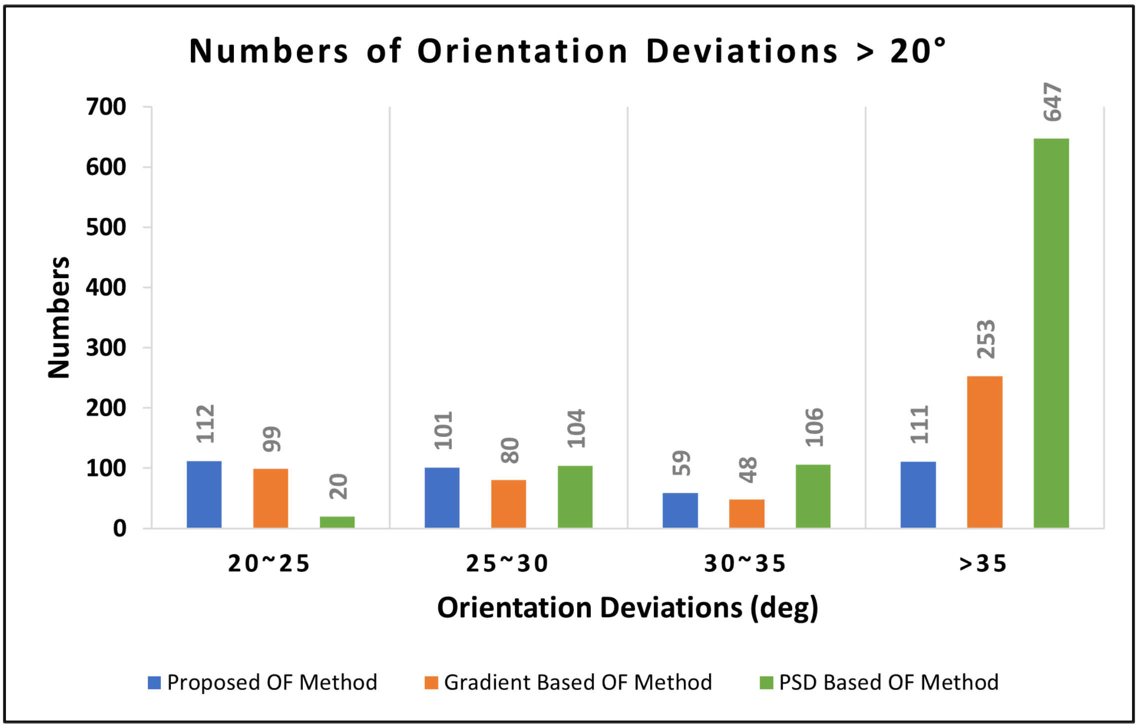

Figure 3.11: Deviations in estimated OF between clear and noisy fingerprint images (1,500 blocks).

doi:10.6342/NTU202302201

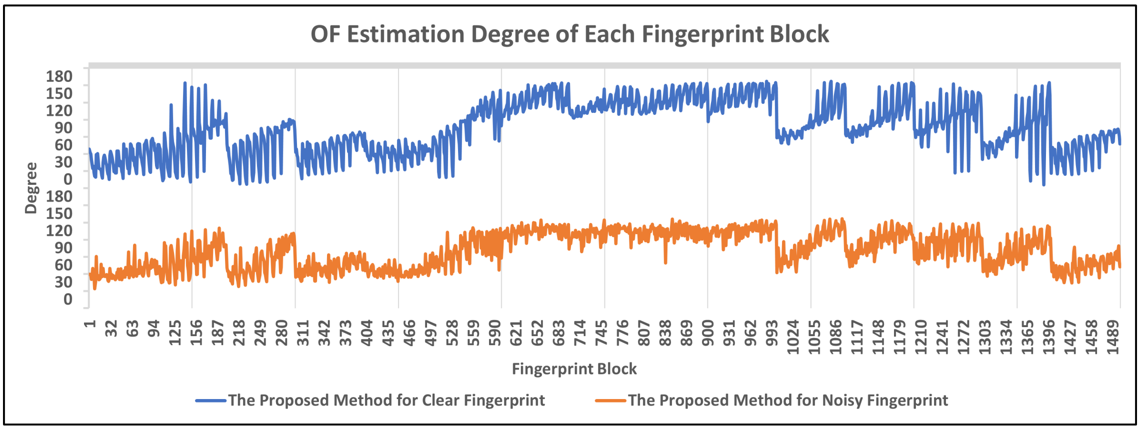

Figure 3.12: OF estimation of each fingerprint block on noisy fingerprint images using the proposed method (1,500 blocks).

doi:10.6342/NTU202302201

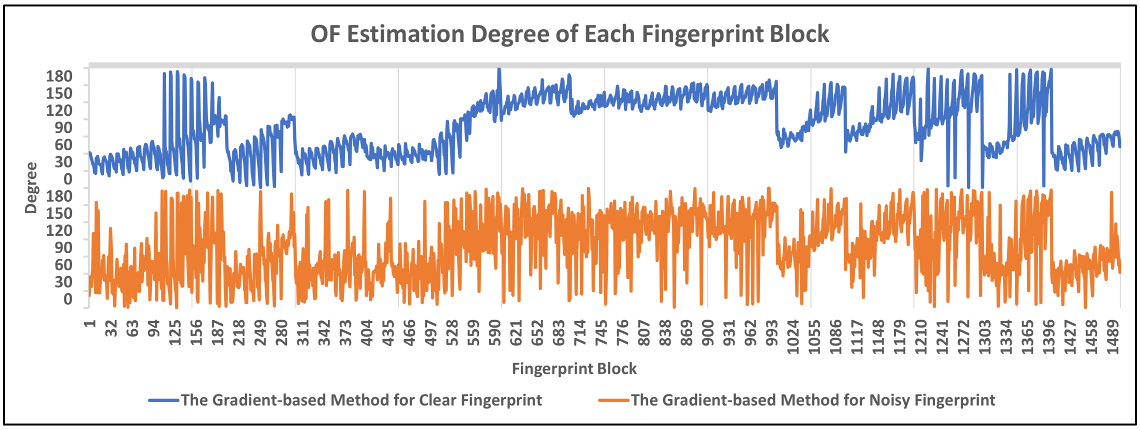

Figure 3.13: OF estimation of each fingerprint block on noisy fingerprint images using the gradient-based method (1,500 blocks).

doi:10.6342/NTU202302201

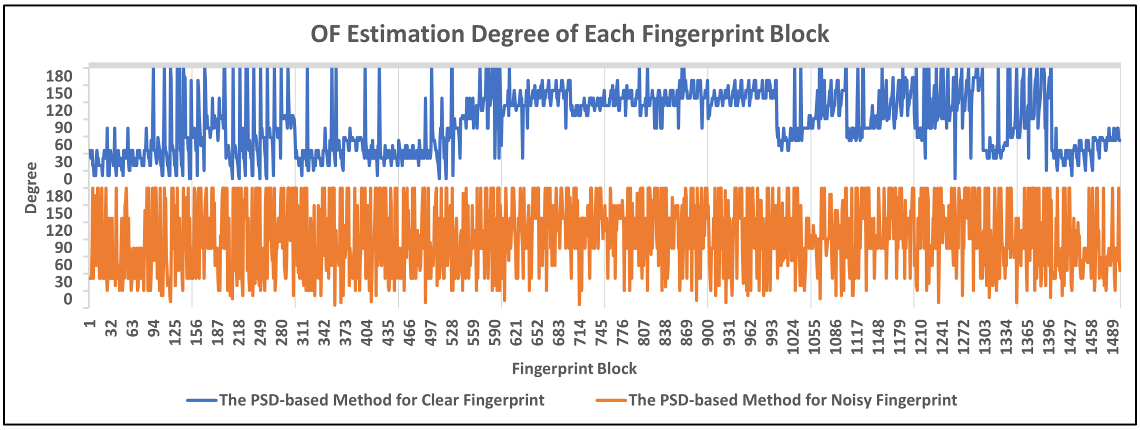

Figure 3.14: OF estimation of each fingerprint block on noisy fingerprint images using the PSD-based method (1,500 blocks).

doi:10.6342/NTU202302201

Table 3.1: The performance of the proposed OF estimation method, the gradient-based method, and the PSD-based method on blurred and noisy fingerprint images.

	The Proposed OF estimation	**The gradients-based OF estimation**	**The PSD-based OF estimation**
Numbers of Deviations > 20° in blurred fingerprint images	7	13	126
Accuracy in blurred fingerprint images	99.53%	99.13%	91.6%
Average deviations in blurred fingerprint images	1.81°	2.18°	6.92°
Correlation coefficient between clear and blurred fingerprint images	0.995	0.978	0.868
Numbers of Deviations > 20° in noisy fingerprint images	383	480	877
Accuracy in noisy fingerprint images	74.46%	68%	41.53%
Average deviations in noisy fingerprint images	13.86°	21.79°	42.19°
Correlation coefficient between clear and noisy fingerprint images	0.868	0.661	0.236

doi:10.6342/NTU202302201

Table 3.2: Advantages and disadvantages of the proposed method and the classic OF estimation methods.

	The Proposed OF estimation method	**The gradients-based OF estimation method**	**The PSD-based OF estimation method**
Advantages	Much higher reliability in blurred and noisy fingerprint images	High accuracy and resolution in clear fingerprint images	Lower computational time than the proposed algorithm.
Disadvantages	Longer computational time demand	Lower reliability in blurred and noisy fingerprint images	Worst reliability in blurred and noisy fingerprint images

doi:10.6342/NTU202302201

doi:10.6342/NTU202302201

Chapter 4 Conclusions

Fingerprint identification technologies are widely used for various applications, including access control systems, forensic investigations, and border security. However, low-quality fingerprint images often inhibit accurate fingerprint feature extraction, classification, and recognition. Therefore, advanced image processing techniques, such as the Gabor filter, are necessary for enhancing image sharpness and reducing noise in fingerprint images. These techniques require a reliable orientation field estimation.

In this study, we propose an effective fingerprint OF estimation method based on grayscale intensity. We conduct experiments to compare the proposed OF estimation algorithm with the gradient-based method and the PSD-based method, which are commonly used for OF estimation. Our experimental results in clear fingerprint images show that the orientation field estimated by the proposed OF estimation algorithm and the gradient-based method are similar, with only 67 blocks out of a total of 1,500 blocks showing a deviation of more than 20 degrees between the two results. The proposed algorithm achieves a higher accuracy rate of 95.53% compared to the result of the PSD-based method which is 92.06%.

Furthermore, we test the reliability of the proposed OF estimation method in blurred and noisy fingerprint images, which often occur in real-world scenarios. In blurred fin-

doi:10.6342/NTU202302201

gerprint images, the OF estimation reliability of the proposed method is 0.4% and 7.93% higher than the gradient-based method and the PSD-based method, respectively. In noisy fingerprint images, the OF estimation reliability of the proposed method is 6.46% and 32.93% higher than the gradient-based method and the PSD-based method, respectively. These results suggest that the proposed algorithm is much more reliable in estimating OF in blurred and noisy fingerprint images than the two commonly used methods.

We attribute the efficient performance in low quality fingerprint images of the proposed algorithm to the fact that it uses convolution to obtain OF, which uses only addition and multiplication, whereas The gradient-based method requires gradient calculation to obtain OF, where the gradient calculation involves division and makes it more susceptible to noises.

In conclusion, our proposed fingerprint OF estimation method based on grayscale intensity achieved high accuracy and reliability in estimating OF in both blurred and noisy fingerprint images. This method has the potential to improve the performance of fingerprint recognition systems, especially in real-world scenarios where image quality is often compromised.

doi:10.6342/NTU202302201

Chapter 5 Future Work

In our study, we conduct a comprehensive comparison between the proposed orientation field estimation algorithm and classical methods, namely the gradient-based and the PSD-based methods. We design and conduct a series of experiments to evaluate the accuracy and reliability of the different algorithms, particularly under challenging conditions such as blurred and noisy fingerprints.

The results of our experiments confirm that our proposed OF estimation algorithm outperforms the classical algorithms in terms of reliability for lower quality fingerprints. We observe that our method consistently produces more accurate and robust OF estimates, even in the presence of blurring or noise in the fingerprint images. However, despite these promising results, the discussion on the underlying reasons behind the observed improvements is not yet complete and requires further investigation.

In our future work, we plan to conduct additional experiments to propose clearer explanations for the observed improvements in our method's performance. This could involve conducting further analyses of the algorithm's mathematical properties, investigating the effects of varying parameter settings, and examining the algorithm's performance on different datasets. We also plan to compare our method with other state-of-the-art OF estimation algorithms, including those based on deep learning techniques.

doi:10.6342/NTU202302201

Furthermore, considering the rapid advancements in AI technology, particularly in the field of deep learning, we aim to explore the development of a deep learning-based approach for fingerprints OF estimation in our future work. Deep learning techniques, such as convolutional neural networks (CNNs), have shown great potential in various image processing tasks, including fingerprint analysis. By leveraging the power of deep learning, we plan to develop a deep learning-based approach for fingerprints orientation field estimation. To validate the strengths and weaknesses of deep learning-based approach, compared to traditional algorithms, we plan to conduct rigorous experiments on large datasets, including diverse fingerprint images with varying quality levels. This will allow us to thoroughly evaluate the performance of deep learning-based approaches, assess their limitations, and gain insights into their potential applications in fingerprints OF estimation.

doi:10.6342/NTU202302201

References

[1] A. F. Abate, M. Nappi, D. Riccio, and G. Sabatino. 2d and 3d face recognition: A survey. Pattern recognition letters, 28(14):1885–1906, 2007.

[2] H. H. Ahmed, H. M. Kelash, M. Tolba, and M. Badwy. Fingerprint image enhancement based on threshold fast discrete curvelet transform (fdct) and gabor filters. International Journal of Computer Applications, 110(3):33–41, 2015.

[3] Z. Alqadi, M. Abuzalata, Y. Eltous, and G. M. Qaryouti. Analysis of fingerprint minutiae to form fingerprint identifier. JOIV: International Journal on Informatics Visualization, 4(1):10–15, 2020.

[4] M. Altarawneh, L. C. Khor, W. L. Woo, and S. S. Dlay. A non reference fingerprint image validity via statistical weight calculation. Journal of Digital Information Management, 5(4), 2007.

[5] A. I. Awad. Fast fingerprint orientation field estimation incorporating general purpose gpu. In Soft Computing Applications, pages 891–902. Springer, 2016.

[6] A. M. Bazen and S. H. Gerez. Directional field computation for fingerprints based on the principal component analysis of local gradients. In Proceedings of ProRISC2000, 11th Annual Workshop on Circuits, Systems and Signal Processing, pages 215–222. Veldhoven, the Netherlands, 2000.

doi:10.6342/NTU202302201

[7] A. M. Bazen and S. H. Gerez. Systematic methods for the computation of the directional fields and singular points of fingerprints. IEEE transactions on pattern analysis and machine intelligence, 24(7):905–919, 2002.

[8] J. Berry and D. A. Stoney. The history and development of fingerprinting. Advances in fingerprint Technology, 2:13–52, 2001.

[9] W. Bian, D. Xu, Q. Li, Y. Cheng, B. Jie, and X. Ding. A survey of the methods on fingerprint orientation field estimation. IEEE Access, 7:32644–32663, 2019.

[10] K. Cao and A. K. Jain. Automated latent fingerprint recognition. IEEE transactions on pattern analysis and machine intelligence, 41(4):788–800, 2018.

[11] R. Cappelli. Fast and accurate fingerprint indexing based on ridge orientation and frequency. IEEE Transactions on Systems, Man, and Cybernetics, Part B (Cybernetics), 41(6):1511–1521, 2011.

[12] K. Ciezar and M. Pochylski. 2d short-time fourier transform for local morphological analysis of meibomian gland images. Plos one, 17(6):e0270473, 2022.

[13] S. Dyre and C. Sumathi. Reliable orientation field estimation of fingerprint based on adaptive neighborhood analysis. ICTACT Journal on Image & Video Processing, 7(3), 2017.

[14] M. Galar, J. Derrac, D. Peralta, I. Triguero, D. Paternain, C. Lopez-Molina, S. García, J. M. Benítez, M. Pagola, and E. Barrenechea. A survey of fingerprint classification part ii: Experimental analysis and ensemble proposal. Knowledge-Based Systems, 81:98–116, 2015.

[15] C. Gottschlich, P. Mihailescu, and A. Munk. Robust orientation field estimation

doi:10.6342/NTU202302201

and extrapolation using semilocal line sensors. IEEE Transactions on Information Forensics and Security, 4(4):802–811, 2009.

[16] L. Hong, Y. Wan, and A. Jain. Fingerprint image enhancement: Algorithm and performance evaluation. IEEE transactions on pattern analysis and machine intelligence, 20(8):777–789, 1998.

[17] U. S. F. B. o. Investigation. The Science of Fingerprints: Classification and Uses. US Department of Justice, Federal Bureau of Investigation, 1984.

[18] A. Jain, A. Ross, and S. Prabhakar. Fingerprint matching using minutiae and texture features. In Proceedings 2001 International Conference on Image Processing (Cat. No. 01CH37205), volume 3, pages 282–285. IEEE, 2001.

[19] A. K. Jain, A. Ross, and S. Prabhakar. An introduction to biometric recognition. IEEE Transactions on circuits and systems for video technology, 14(1):4–20, 2004.

[20] H. Kekre and V. Bharadi. Fingerprint orientation field estimation algorithm based on optimized neighborhood averaging. In 2009 Second International Conference on Emerging Trends in Engineering & Technology, pages 228–234. IEEE, 2009.

[21] H. Li, T. Wang, Y. Tang, J. Wu, P. Yu, L. Guo, J. Chen, and Y. Zhang. Combining multi-scale composite windows with hierarchical smoothing strategy for fingerprint orientation field computation. Biomedical engineering online, 17(1):1–21, 2018.

[22] L.-m. Liu and T.-S. Dai. Ridge orientation estimation and verification algorithm for fingerprint enhancement. J. Univers. Comput. Sci., 12(10):1426–1438, 2006.

[23] D. Maltoni, D. Maio, A. K. Jain, and S. Prabhakar. Handbook of fingerprint recognition. Springer Science & Business Media, 2009.

doi:10.6342/NTU202302201

[24] O. Marques. Practical image and video processing using MATLAB. John Wiley & Sons, 2011.

[25] D. H. McMahon, G. L. Johnson, S. L. Teeter, and C. G. Whitney. A hybrid optical computer processing technique for fingerprint identification. IEEE Transactions on Computers, 100(4):358–369, 1975.

[26] R. Medina, J. Llamas, J. Gómez-García-Bermejo, E. Zalama, and M. J. Segarra. Crack detection in concrete tunnels using a gabor filter invariant to rotation. Sensors, 17(7):1670, 2017.

[27] Y. Mei, H. Sun, and D. Xia. A gradient-based combined method for the computation of fingerprints' orientation field. Image and Vision Computing, 27(8):1169–1177, 2009.

[28] D. Mukherjee and A. Das. Gabor Filter Based Automated Enhancement of Brain Tumors, pages 71–80. Springer, 2021.

[29] E. Newham, C. Bunney, and C. Mearns. The biometrics report, sjb services. New York, pages 269–302, 1995.

[30] M. d. A. Oliveira and N. J. Leite. A multiscale directional operator and morphological tools for reconnecting broken ridges in fingerprint images. Pattern Recognition, 41(1):367–377, 2008.

[31] C. H. Park and H. Park. Fingerprint classification using fast fourier transform and nonlinear discriminant analysis. Pattern Recognition, 38(4):495–503, 2005.

[32] Z. Qu, J. Liu, Y. Liu, Q. Guan, C. Yang, and Y. Zhang. Orienet: A regression system

doi:10.6342/NTU202302201

for latent fingerprint orientation field extraction. In International Conference on Artificial Neural Networks, pages 436–446. Springer, 2018.

[33] K. Raja. Fingerprint recognition using minutia score matching. arXiv preprint arXiv:1001.4186, 2010.

[34] N. K. Ratha, S. Chen, and A. K. Jain. Adaptive flow orientation-based feature extraction in fingerprint images. Pattern recognition, 28(11):1657–1672, 1995.

[35] N. K. Ratha, K. Karu, S. Chen, and A. K. Jain. A real-time matching system for large fingerprint databases. IEEE transactions on pattern analysis and machine intelligence, 18(8):799–813, 1996.

[36] R. P. Sharma and S. Dey. Fingerprint liveness detection using local quality features. The Visual Computer, 35(10):1393–1410, 2019.

[37] F. Turroni, D. Maltoni, R. Cappelli, and D. Maio. Improving fingerprint orientation extraction. IEEE Transactions on Information Forensics and Security, 6(3):1002–1013, 2011.

[38] Y. Wang, J. Hu, and F. Han. Enhanced gradient-based algorithm for the estimation of fingerprint orientation fields. Applied Mathematics and Computation, 185(2):823–833, 2007.

[39] L. Wieclaw. Gradient based fingerprint orientation field estimation. Journal of Medical Informatics & Technologies, 22, 2013.

[40] J. Yang, L. Liu, T. Jiang, and Y. Fan. A modified gabor filter design method for fingerprint image enhancement. Pattern Recognition Letters, 24(12):1805–1817, 2003.

doi:10.6342/NTU202302201

doi:10.6342/NTU202302201

Appendix — Biography and Publication

.1 Biography

Ting-Wei Shen received M.S. degrees in Electro-Optical Engineering from National Taiwan Normal University in 2012. He is currently pursuing his Ph.D. at the National Taiwan University in Mechanical Engineering Department and pass the qualifying exam in 2019/09/05. His current research interests include Image Quality Assessment Algorithm, Image Orientation Field Estimation, Micro/Mini LED Display Technology, Auto Testing with Machine Vision.

.2 Publication

[1] Shen, T. W., Hsu, M. H., Shen, C. H., Wu, W. F., Lu, Y. C., & Chu, C. C. (2023). An effective fingerprint orientation field estimation method using differential values of grayscale intensity. PeerJ Computer Science, 9, e1342.

[2] Shen, C. H., Shen, T. W., Hsieh, T. Y., Lan, K. C., Hsu, S. H., Wang, C. H., ... & Tseng, Z. L. (2023). The Enhanced Thermal Stability of (Mg0. 95Ni0. 05) 2TiO4

doi:10.6342/NTU202302201

Dielectric Ceramics Modified by a Multi-Phase Method. Materials, 16(8), 2997.

[3] Shen, T. W., Li, C. C., Lin, W. F., Tseng, Y. H., Wu, W. F., Wu, S., ... & Hsu, M. H. (2022). Improving Image Quality Assessment Based on the Combination of the Power Spectrum of Fingerprint Images and Prewitt Filter. Applied Sciences, 12(7), 3320.

[4] Tsai, C. T., Shen, T. W., Chen, Y. P., & Hsu, P. H. (2018, December). Control strategy of PV/diesel/battery hybrid system for island-based microgrid. In 2018 International Symposium on Computer, Consumer and Control (IS3C) (pp. 121-124). IEEE.

[5] Lee, M. H., Hsu, S. M., Shen, J. D., & Liu, C. (2015). Stress distribution of IGZO TFTs under mechanical rolling using finite element method for flexible applications. Microelectronic Engineering, 138, 77-80.

doi:10.6342/NTU202302201